Estimation and Modeling of Damping and Engineering Auxiliary Damping Systems in Civil Engineering Structures: An Overview

Tracy Kijewski and Ahsan Kareem
NatHaz Modeling Laboratory
University of Notre Dame

TABLE OF CONTENTS

1 Introduction

As the height and flexibility of the modern skyscraper increases, so too does the structure's response to dynamic wind loads. In general, the level of these oscillations is not significant enough to cause structural damage. However, strong winds frequently cause perceptible vibrations in the building, which can cause anxiety and discomfort to the building's occupants. The external manifestations of the human response to this swaying motion are varied and will differ from person to person. However, some of the most common symptoms include dizziness, headaches, and nausea.

To limit these negative responses, the wind-induced response of tall buildings is frequently controlled by global design modifications that include the provision of additional damping. An increase in the damping of a structure results in a corresponding decrease in structural motion. Although there four sources of structural damping: structural, aerodynamic, soil, and inherent damping, indirect damping currently offers the most promising prospects for controlling building motion.

During the design phase of a building, the level of damping that will be in the building following construction must be determined to aid in the design of control techniques. However, unlike easily quantifiable properties like mass and stiffness, the level of damping is an ambiguous quantity. It can vary with the amplitude of the excitation and depends upon complex mechanisms within the structure, many of which are not fully understood. The demand for accurate pre-construction damping is urgent. However, significant challenges face the engineering community as they search for reliable techniques for estimating these values. This paper first discusses the two primary types of damping that occur in a structure: structural and aerodynamic. The techniques that are currently available for estimating these types of damping in a structure are then discussed. In addition, the advantages and shortcomings of these techniques are presented.

Because the actual damping level of a building is difficult to measure prior to construction, some researchers have suggested that a database be created which contains reliable, high-quality data from existing buildings of varying types and conditions (Tamura et al., 1996). Such a database would aid in the development predictors damping ratios at the design stage. This paper presents one such proposed database and discusses the necessity and quality of its data.

After the damping of a building has been estimated, a control system may be designed that will best limit the motion of the building. This paper discusses various auxiliary control methods that are currently being incorporated into buildings to augment their inherent damping. These devices can be divided into three categories: passive, active (and hybrid), and semi-active. Passive devices increase the damping of a system by modifying the frequency response of the system, thereby reducing the structural response. The most commonly used passive devices include tuned mass dampers (TMDs) and tuned liquid dampers (TLDs), which include sloshing dampers (TSDs) and tuned liquid column oscillation-type dampers (TLCDs). In contrast, active control devices limit the structural response using an external energy source. The most common active devices are the active mass damper (AMD) and the active bracing system (ABS). A semi-active system is a

combination of active and passive devices, which avoids the shortcomings that are inherent in either system when used alone.

Finally, this paper will discuss the design and inclusion of such damping systems. This discussion will present techniques for adding damping devices to buildings and placing such devices in the structure.

2 Modeling and Estimation of Damping

As the height and flexibility of modern buildings continues to increase, the need for a better understanding of the dynamic behavior of these buildings also increases. A critical concern in the design of tall buildings is that the building must have sufficient damping to withstand the dynamic loads brought upon it by the wind so that the habitability of the building is not compromised. Therefore, the ability to estimate the damping of a system prior to construction is necessary to insure the structure satisfies habitability criteria and allow for the inclusion of a damping control device, if needed. However, unlike the mass and stiffness characteristics of a structural system, damping does not relate to a unique physical phenomenon. The level of damping is an ambiguous quantity. It can vary with the amplitude of the excitation and depends upon complex mechanisms within the structure, many of which are still not fully understood. Despite the urgent need for accurate damping estimates in design, there is still no one technique for estimating these values (Kareem and Gurley, 1995).

Structural damping is a measure of energy dissipation in a vibrating structure that results in bringing the structure to a quiescent state. The damping capacity is defined as the ratio of the energy dissipated in one oscillation cycle to the maximum amount of energy accumulated in the structure in that cycle. There are as many structural damping mechanisms as there are modes of converting mechanical energy into heat. The most important mechanisms are material damping and interfacial damping (Nashif et al., 1984).

The material damping contribution is the result of a complex molecular interaction within the building material. Therefore, material damping is dependent on the type of material, the methods used in manufacturing the material, and the final finishing processes. The complexity of the situation is further enhanced by the fact that material properties often differ from sample to sample, which could result in significant differences in energy losses among distinct members of a structural system. In addition, the equations of motion in structural dynamics usually describe macroscopic behavior, while material damping processes arise from microscopic phenomena. This conflict leads to a search for phenomenological theories for the representation of structural damping.

In contrast, the interfacial damping mechanism results from Coulomb friction between members and connections of a structural system and between structural components like partitions and exterior facades. Welded connections tend to reduce the contribution of interfacial damping more than bolted connections. Soil structure interaction also contributes towards the overall damping, depending on the soil characteristics (Novak, 1974; Wolf, 1988).

Unlike structural damping, aerodynamic damping is experienced by a structure vibrating in air. In general, the aerodynamic damping contribution is quite small compared to mechanical damping in a structure, and it is positive in low to moderate reduced wind speeds (i.e., speed normalized by frequency and body width). However, at certain wind speeds, negative aerodynamic damping may occur.

Nonlinearities in either the loading or the structural systems further complicate the estimation of damping levels. Nonlinearity effects, in combination with nonstationary features of full-scale observations under winds, may affect the accuracy of conventional damping estimation procedures (Jeary, 1992). Nonlinearity in either the loading or a structural system that may couple two orthogonal modes with equal frequencies can indirectly add to the damping in a system as energy transfers from one direction of motion to another (Kareem, 1982). This design feature can indirectly help to augment damping in buildings, provided the two orthogonal modes have the same frequency.

This section discusses the types of damping sources that are available to structures and the estimation of this parameter.

2.1 Structural Damping

In engineering practice, a viscous damping model is typically used because it leads to a linear equation of motion. The viscous damping coefficient is either assigned based on the construction material (e.g., steel or concrete) or is evaluated using a system identification technique. One such technique is a logarithmic decrement of a free vibration test. Any source of nonlinearity is obscured in this approach, and consequences of such an assumed model are either ignored or disregarded. This concept has been extended to represent equivalent viscous damping, whereby the energy dissipated by a nonlinear system in a steady-state vibration is equated to the energy dissipated by an equivalent viscous system.

2.1.1 Damping Models

Some of the commonly used damping models can be described by:

$$f_d(x,\dot{x}) = a\dot{x}\left|\dot{x}\right|^{q-1} \tag{1}$$

where $f_d(x,\dot{x})$ is the damping force and a is the damping coefficient. The value of q determines the damping model as follows.

For linear viscous damping (q = 1):

$$f_d(x,\dot{x}) = c\dot{x}\,. \tag{2}$$

For Coulomb damping (q = 0):

$$f_d(x,\dot{x}) = m\frac{\dot{x}}{|\dot{x}|} = m\,sign(\dot{x}). \tag{3}$$

For quadratic damping (q = 2):

$$f_d(x,\dot{x}) = q\dot{x}|\dot{x}|. \tag{4}$$

The ratios of the equivalent viscous damping for these cases are given as follows.

For viscous damping:

$$\frac{c}{2mw}. \tag{5}$$

For Coulomb damping:

$$\frac{2m}{pmw^2A}. \tag{6}$$

For quadratic damping:

$$4q\frac{A}{3pm}. \tag{7}$$

For general n[th] power damping:

$$\frac{1}{2}\frac{a}{m}g\,(Aw)^{q-1} \tag{8}$$

where $g = \dfrac{2\Gamma\left(\frac{1}{2}(q+2)\right)}{\sqrt{p}\,\Gamma\left(\frac{1}{2}(q+3)\right)}$ and $G(\ )$ denotes the Gamma function; c is the viscous damping coefficient; q is the quadratic damping coefficient; m is the Coulomb damping coefficient; and A is the amplitude of motion.

It is important to note that the linear viscous damping ratio is independent of amplitude, whereas the Coulomb and quadratic damping ratios are inversely and directly proportional to amplitude of motion. For a lightly damped system, where all three preceding damping mechanisms may be present, a first-order approximation for the total damping present in the system can be obtained by fitting data to Eq. 1. Such a model may bring out useful information regarding the inherent damping mechanisms in a system that experiences different types of damping sources (e.g., an

offshore platform or a building whose damping is amplitude dependent). Novak (1971) offers a number of techniques to quantify parameters of nonlinear vibration systems.

Estimates of the model parameters are obtained by a least square fit of the data. Other models such as "stick-slip" type models, elasto-plastic, and bilinear models can be invoked to describe the variation in the system damping with amplitude. In the case of steel buildings, such models can describe the dissipation of energy in frictional modes such as in-filled panels and partitions and between structural framing and cladding. In the case of uncracked concrete structures, purely viscous damping occurs. For cracked concrete structures, both frictional damping, which is due to friction between the concrete and reinforcing steel in the cracked tension zone, and viscous damping in the compression zone are present. A concrete element may be modeled by a spring oscillator with a viscous dashpot and a stick-slip element.

2.1.2 Full-Scale Measurements and Damping in the Fundamental Mode

The selection of an appropriate value of damping is a subject of controversy in design practice. Using current state-of-the-art procedures in the design of tall buildings only allows the designers to predict structural damping to plus or minus 30% until the building is completed. This estimate is essentially obtained using knowledge gleaned from existing buildings of similar material and structural systems on which tests have been conducted. Although it is generally agreed that damping values change with amplitude of motion, their fundamental descriptions are rather uncertain and limited. In addition to the complex nature of damping mechanisms, the methods used to determine the damping of full-scale structures and the analysis and interpretation of such data introduce additional uncertainty. Assessment of damping in full-scale structures has been undertaken by several investigators. A sampling of such studies can be found in Yokoo and Akiyama (1972), Trifunac (1972), Hart and Vasudevan (1975), Raggett (1975), Taoka et al. (1975), Hudson (1977), Jeary and Ellis (1981) and Celebi and Safak (1991). Information available from full-scale experiments has been assembled by Yokoo and Akiyama (1972), Haviland (1976), Jeary and Ellis (1981), Davenport and Hill-Carroll (1986), Jeary (1986), Lagomarsino (1993), and Tamura et al. (1994), among others.

Haviland (1976) reported a wide range of data for different levels of response amplitudes in a variety of structural systems and building heights. This study showed that the log-normal and Gamma distributions provided the best fit to the damping variations. The coefficient of variation (COV) of the damping estimates based on this data set varied from 42% to 87%. Davenport and Hill-Carroll (1986) reexamined the database and noted that the COV ranged from 33% to 78% and suggested a value of 40%. Based on measured data, ESDU (1983), Jeary (1986), Lagomarsino (1993), and Tamura et al. (1995) established expressions for the damping ratio variation as a function of the structural displacement level. It is important to note that most of these databases have a large overlap of information since they contain many common buildings.

A review of the database that has led to carefully selected expressions for the damping variation as a function of amplitude suggests that the data mostly concerns mid-rise buildings with a maximum height of approximately 20 stories. As a result, there is a serious scarcity of data for high-rise buildings that are taller than 20 stories. This lack of data is especially serious for amplitudes that are related to earthquake-induced responses, which generally provide much higher damping

estimates than those available for wind-excited structures. More importantly, it is above this height that the wind-excited resonant portion of the structural response begins to dominate the background (i.e., nonresonant) portion. It is this resonant response component that is influenced by damping, regarding which little information is available. In Davenport and Hill-Carroll (1986), a summary of damping estimates versus amplitudes clearly demonstrates the scarcity of available data. In their database for buildings over 20 stories, damping estimates are available for acceptable levels of motion for human comfort. In addition, the database contains some data points for the transition region in which the building height determines the level of acceptability. However, not a single data set exists for unacceptable acceleration levels with a mean recurrence interval of 10 years. It is these last two levels of motion that are of interest to designers of tall buildings. A similar lack of information exists in the data set reported by Lagomarsino (1993) for buildings with periods larger than 3 seconds. Jeary (1986) very carefully scrutinized this damping database and eliminated a majority of the measured damping data due to concerns such as a lack of documentation and an absence of variance errors and confidence intervals. The remaining database, which was used for developing the model, was again biased toward mid-rise buildings, with the exception of the Transamerica building. The predictor model, however, agrees well with the general concept that the damping values reduce with an increase in the building height or period. The model in Lagomarsino (1993) exhibits an opposing trend in that a larger period results in larger damping. With a few notable exceptions, this contradicts most full-scale measurements reported in the literature.

2.1.3 Damping in Higher Modes

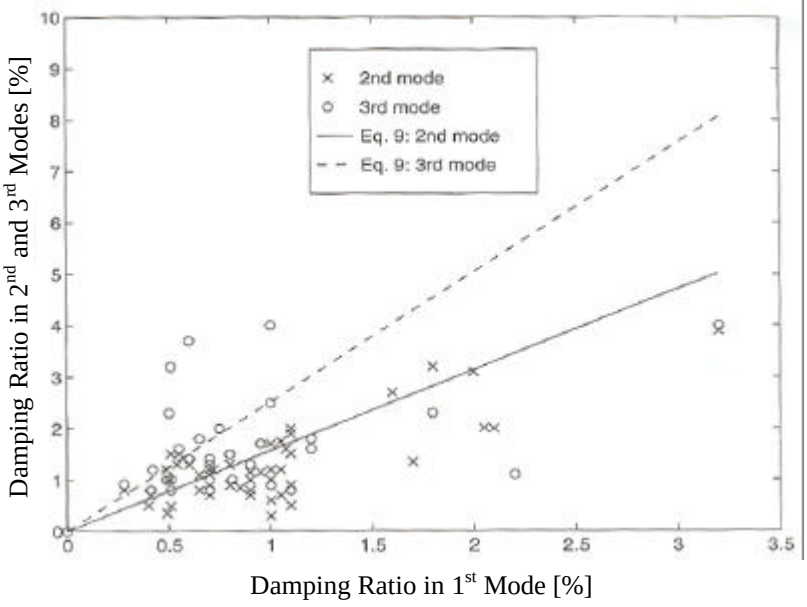

Figure 1: Comparison of measured damping estimates and expression in Eq. 9 *(taken from Kareem and Gurely, 1995).*

Damping in the fundamental mode is very low, which indicates that very little energy is dissipated by structural connections and that most of the building structure deforms as a rigid body. However, it is expected that in higher modes a building will experience more flexural and shear deformation, which may contribute to higher damping. Also, radiation damping due to the soil-structure interaction may contribute to higher damping (Novak, 1974). Because of the scarcity of reliable damping data in the fundamental mode, information on damping in higher modes becomes even scarcer and less reliable. However, the contribution of higher modes must be included when estimating the building acceleration to appraise serviceability limit states. Kareem (1981) noted that for the acrosswind acceleration response of a square cross-section building, the contribution of the second mode is approximately 13%. Neglecting such contributions

may impact the serviceability of a building. O'Rourke (1976) discussed a paper by Saul and Jayachandran (as referenced in O'Rourke) that concerned the importance of modes to the total acceleration response and examined values of damping in higher modes. Saul and Jayachandran assumed that the damping in higher modes was lower than in the first mode, which may have resulted in an overemphasis on the relative importance of higher modes. O'Rourke analyzed the data available in the literature and noted that in 61% of the cases selected, the damping in the second mode was higher than the damping in the first mode. The corresponding value for the third mode was found to be 53%. The average value of the ratio between the second and first mode damping was 1.39, and the average value of the ratio between the third and the first modes was 1.61.

Unlike Saul and Jayachandran's assumption, Kareem (1981) assumed that the damping was proportional to the stiffness, which increases in higher modes. Accordingly, the damping in higher modes was given by:

$$\frac{x_n}{x_1} = 1 + C\left(\frac{f_n}{f_1} - 1\right), \tag{9}$$

where C is a constant that is approximately equal to 0.38 based on the data available in Yokoo and Akiyama (1972) and f represents the frequency in the mode given by the subscript. In Figure 1, the database from the study by Tamura et al. (1994) and other sources was utilized to examine the applicability of the expression in Eq. 9 in light of the additional data. Note that the database is restricted to steel buildings with a height greater than 20 stories under the light to moderate levels of oscillations generally experienced in typical wind conditions. In view of the general variability of damping, which is further compounded by the higher modes, the expression in Eq. P01E09 appears to portray a satisfactory representation of the general trend.

2.2 Aerodynamic Damping

The equation of motion of an aerodynamically excited structure is given by:

$$M\ddot{X} + 2wMx_s\dot{X} + Mw^2X = F(t, X, \dot{X}, \ddot{X}). \tag{10}$$

The left hand side of the equation represents typical inertial, damping and stiffness forces acting on the structures, whereas the right hand side of the equation denotes the aerodynamic forcing function that is dependent on time, space and its derivatives. Typically $\ddot{X}$ and X are known to have an insignificant influence on the building response due to the relatively small value of the aerodynamic mass and stiffness in comparison with that of the building. It is the $\dot{X}$ term which, depending on its sign, contributes positive or negative values of aerodynamic damping on structures. Since the aerodynamic damping is due to building motion, it is manifested in the alongwind, acrosswind and torsional directions. There are two approaches to quantify aerodynamic damping, namely, quasi-steady or unsteady aerodynamics of buildings. These are described below.

2.2.1 Quasi-Steady Aerodynamics

For a long time, aerodynamic damping has been evaluated with respect to the galloping phenomenon. In this technique, the concept of quasi-steady theory is invoked. It essentially implies that for every instant during an oscillation, the aerodynamic force is the same as the force on a rigid segment of the body at the same angle of attack. This assumption has been shown to hold for large reduced velocities where the wavelengths associated with the frequencies of aerodynamic loading are several times the representative width of the building. In this situation, the approach flow can be assumed to be locally steady. The aerodynamic damping on a segment of a building is determined from sectional aerodynamic characteristics for the corresponding angle of attack in terms of a force coefficient and a relative velocity. The aerodynamic damping in the lateral and torsional directions based on the quasi-steady theory are given by

$$x_x^a = \frac{3}{4p(3+a)} \frac{g_a}{g_b} \frac{V_n}{f_x d} C_{F_x} \tag{11}$$

$$x_y^a = \frac{3}{8p(3+a)} \frac{g_a}{g_b} \frac{V_n}{f_y d} \frac{dC_{F_y}}{dq} \tag{12}$$

$$x_z^a = -\frac{3}{8p(3+a)} \frac{g_a}{g_b} \frac{V_n}{f_q d} \frac{rb}{r_m^2} \frac{dC_{F_x}}{dq} \tag{13}$$

where a is the power law exponent; g_a are g_b the air and building specific weights; C_{Fx}, C_{Fy}, and C_{Fq} are the force coefficients in the *x, y and q* directions, respectively; f_x, f_y, and f_q are the natural frequencies in their respective subscript directions; d is the body width; r is the distance of the leading edge from the building centroid; r_m and is the mass radius of gyration (Kareem, 1978). The preceding expressions utilize linear mode shapes in all three directions.

As noted earlier, the quasi-steady theory is generally not applicable in the low reduced velocity range that corresponds to the operational velocities of typical buildings in wind. Therefore, the evaluation of aerodynamic damping must be based on unsteady aerodynamics. This can be accomplished through a free oscillation or forced oscillation test.

2.2.2 Unsteady Aerodynamics

The importance of evaluating aerodynamic damping has increased with the advent of aerodynamic models, which utilize high-frequency base balances. There have been a number of reported studies concerning the measurement of aerodynamic loads on structures using a wide variety of force balances. However, Saunders and Melbourne (1975) were the first to carry out a measurement program that resulted in a host of force spectra acting on a wide range of building cross-sections. They also concluded that the non-dimensional crosswind force spectra on the types of buildings tested were insensitive to the level of motion of the buildings for reduced velocities up to at least 10. In other words, the aeroelastic effects or aerodynamic damping could be neglected. Kareem (1978) conducted a validation study of the crosswind spectra that was derived from statistical

integration of surface pressures. In this study, it was noted that the response estimates computed using the measured spectra began to depart from the estimated values based on the aeroelastic model test of the same building at reduced velocities above 6. The predicted values of the response for reduced velocities greater than 6 tended to under-predict the aeroelastic measurements. This suggested that a contribution from the motion-induced effects was missing since it had automatically been accounted for in the aeroelastic case. The damping estimates from the aeroelastic model suggested a constant increase in the negative aerodynamic damping. By including the negative aerodynamic damping, the response predictions provided a better comparison with the aeroelastic tests at higher reduced velocities. However, some discrepancies remained unresolved at intermediate reduced velocities (Kareem, 1982). It appears that simply attributing all motion-induced effects to aerodynamic damping may be an excessive simplification. The motion of a structure also modifies the flow field around it and particularly enhances the spanwise pressure correlation, which may lead to an increased forcing in comparison with that measured by a force balance.

Following the work of Saunders and Melbourne (1975), Kwok and Melbourne (1981) reported that near the critical reduced velocity, and particularly at low values of structural damping, displacement dependent lock-in excitation was found to be significant, which resulted in large increases in the crosswind response. They suggested including a sinusoidal lock-in excitation model along with a random excitation model to account for the preceding observation. It was suggested that the lock-in effects become important when the ratio of the building's top displacement to its width exceeds 0.025.

Boggs (1992) reported a systematic study that focused on the validation of an aerodynamic model. This topic had been addressed earlier, but the relevant error-controlling parameters had not been clearly identified, nor had the quantitative limits required for valid results on the parameter studies been established. This study, though limited to a slender square building, has provided a clear picture of the consequences of neglecting aeroelastic feedback and defined conditions under which an aerodynamic model is valid. The normalized tip deflection criterion was noted to be a poor indicator of aeroelastic magnification, and the existence of such a critical limit is not justified. Results of this study show that the reduced velocity, in conjunction with the mass damping parameter, provides a good characterization of the aeroelastic magnification factor given by the ratio of the response estimate determined using the aeroelastic model and the aerodynamic model. Boggs' results demonstrate that for the mass damping parameter in the range of typical tall buildings, the motion induced effects may be worth considering for reduced velocities as low as 6. This corroborates observations made by Kareem (1982).

2.2.3 Experimental Identification of Aerodynamic Damping

The experimental identification of aerodynamic forces can be accomplished either by a free or forced vibration test. Using a free vibration test, the change in the frequency and damping of models oscillating in wind are observed. This method has been extensively used to identify motion-dependent aerodynamic forces in bridge aeroelasticity (Scanlan and Tomko, 1971). Kareem (1982) utilized a free vibration approach to assess the aerodynamic damping of building models and chimneys in a wind tunnel. A number of researchers have utilized forced vibration tests to identify the aerodynamic stiffness and damping of two-dimensional models (e.g., Otsuki et

al., 1974). Steckley (1989) used an experimental system for the measurement of motion induced forces on a base pivoted model. This study cataloged variations in the motion-induced force with oscillation amplitude for prisms of different cross-sections. This data was later employed by Watanabe et al. (1995) to fit empirical aerodynamic damping functions for practical applications. Their model is based on real and imaginary parts of the modified complex transfer function of a single degree of freedom (SDOF) oscillator.

2.3 Evaluation of Damping

Damping estimation from a time history of responses can be classified into two categories: spectral and time series approaches. In this section, the following are classified as spectral approaches: logarithmic decrement, spectral half-power method, spectral moment method, spectral curve fitting, and wavelet transform-based spectral estimates. The time series techniques may include maximum entropy estimates, auto-regressive (AR) or auto-regressive and moving-averages (ARMA) techniques (Li and Kareem 1990a), auto-correlation decay, the random decrement method and system identification schemes such as Extended Kalman Filtering.

2.3.1 Spectral Techniques

The infinite harmonic basis functions in Fourier based spectral estimations necessarily introduce errors when applied to finite duration signals. In most spectral-based approaches, it is difficult to obtain sufficient accuracy because of limitations on resolution and high COVs of spectral estimates as longer data sets are needed to improve estimates. By increasing the number of degrees of freedom by merging neighboring spectral estimates and/or ensemble averaging the individual estimates from several realizations, spectral estimates can be improved. However, this approach is marred by the unavoidable presence of nonstationarity concerns that are inherent in long records. Details concerning this issue are present in the literature. Because of the preceding difficulty, attempts to smooth the actual spectral estimates have been made through curve fitting. For example, Breukelman et al. (1993) and Jones and Spartz (1990) fit the spectral estimates to a transfer function of a SDOF system by employing a maximum likelihood estimator and a least squares approach, respectively. By selecting a sample length that is long enough to ensure sufficient frequency resolution, avoiding nonstationarity problems, and ensemble averaging similar records to reduce the variance of spectral estimates, smooth spectra can be obtained for linear systems. However, the characteristic features of nonlinear systems that have transfer functions that depart from linear behavior and the response of systems to nonlinear loading may be obscured in such a curve fitting approach. Similar observations have been made by Jeary (1992).

Wavelet-based spectral estimation offers another alternative since it better represents the true signal energy due to the use of localized basis functions (Gurley and Kareem, 1995). It is shown in Gurley and Kareem (1995) that the wavelet estimator exactly reproduces the signal energy which the Fourier based spectral estimate does not reproduce due to leakage that results in raggedness in the spectral curves. However, the use of orthogonal wavelets does not provide the same resolution in the spectral estimates as Fourier-based approaches, especially at the high frequencies. In contrast, at very low frequencies, the wavelet-based estimates give much better resolution. This can be further improved through a zooming technique or a spectral estimation within an octave by over-sampling, which leads to non-orthogonal wavelets (Gurley and Kareem, 1995).

2.3.2 Time Series Methods

Methods based on a time series approach offer advantages over spectral methods since they eliminate the problems of resolution based on short length of records and questions about the stationarity of long records. These spectral estimates provide smoother curves without the leakage problems associated with the Fourier-based approaches. These leakage problems are significant for short length data sets where the uncertainty principle does not permit good frequency resolution. However, the time series methods are sensitive to the order of the model or the number of coefficients (Li and Kareem, 1990b, 1993). When using an AR model, if the order is small, the dominant peaks may not be resolved. On the other hand, large order systems can introduce spurious peaks that may contaminate the spectral estimate and the variance. An optimal selection of the order results in accurate spectral estimates.

A serendipitous advantage of these time series based models is that the spectrum is readily obtained once the model coefficients are estimated from the time series. Furthermore, the estimation of structural characteristics is also possible from system identification techniques using time series models such as auto-regressive moving average models with exogenous input (ARMAX). In such a case, the system is modeled by an input, output, and noise. The modulus and argument of the poles of the system transfer function are then related to the system damping and frequency (e.g., Safak, 1989).

In the following sections, the efficacy of two other time series methods, the Random Decrement Technique (RDT) and Extended Kalman Filtering for estimating damping will be evaluated through examples.

2.3.3 Examples Using the Random Decrement Technique

The RDT utilizes the resulting signature from the ensemble averaging of segments of the response of a linear system to determine system damping. The requirement of specific initial conditions for each segment in the averaging procedure yields a signature that represents free vibration of the system from specified initial conditions. Damping estimates are then extracted from this Random Decrement Signature (RDS) (Cole, 1973). The total response of a dynamic system (x_T) is a superposition of the response due to both an initial displacement (x_o) and velocity ($\dot{x}_o$) and the response component due to the applied force (x_F):

$$x_T = x_{x_o} + x_{\dot{x}_o} + x_F \,. \tag{14}$$

The goal is to ensemble average samples of response data such that the forced vibration response component reduces to zero, leaving the free vibration response from the specified initial conditions, x_o and $\dot{x}_o$.

The forced vibration response of a linear system due to a zero mean, stationary random input is itself random, zero mean and stationary. As the number of segments increases, the ensemble average of such a process approaches zero, with all segments in the average beginning at the same threshold conditions, which specify both amplitude and slope of the response. One

conceptualization of the RDT is provided in Figure 2, where the components of the signal are ensemble averaged separately to illustrate the progression of the signal from a forced vibration to free vibration decay. In this case, the choice of alternating positive and negative slopes of the captured segments essentially averages out the portion of the response due to the initial velocity condition.

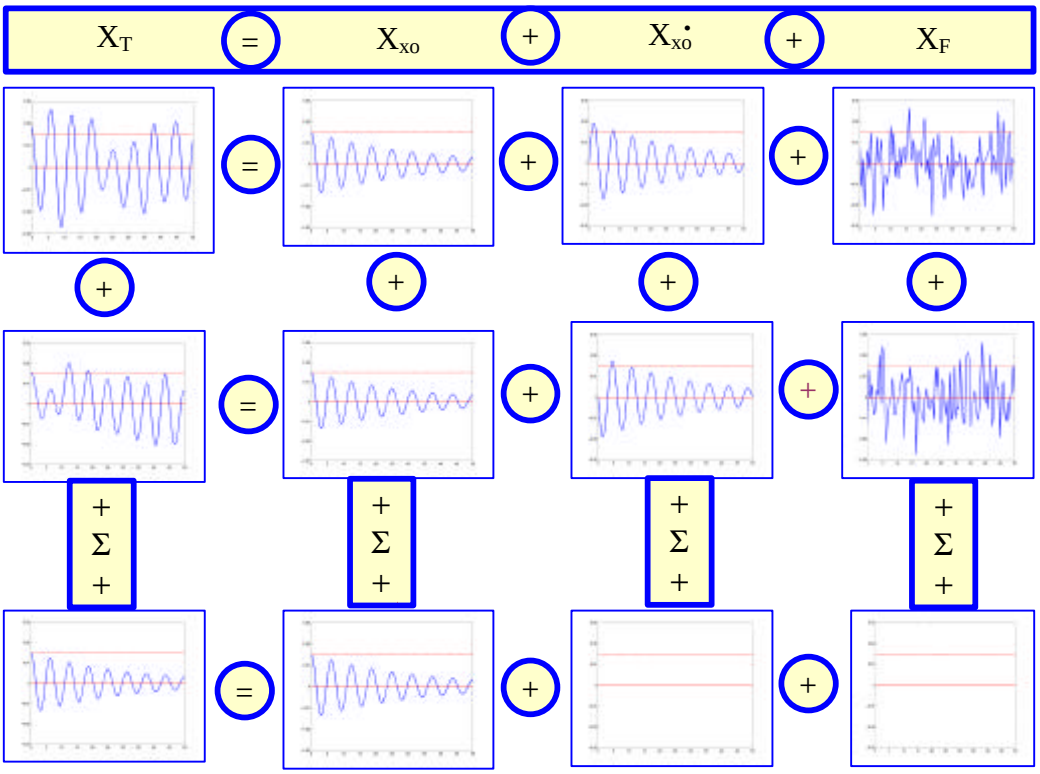

Figure 2: Conceptualization of Random Decrement Technique.

In this instance, the RDS is expressed as follows (Yang et al., 1983):

$$h(t) = \frac{1}{N}\sum_{i=1}^{N} x_i(t_i + t), \tag{15}$$

where $x_i(t_i)$ is the threshold value; N is the number of segments in the ensemble average; and the initial slope flips for each sequential segment. The random decrement signature is defined in the time interval $0 \le t \le g$ where g is the time from the starting point of the last segment to the end of the signal.

This intuitive explanation has been used in much of the available literature and seems to be reasonable for linear systems. The technique has an advantage over the use of autocorrelation or spectral methods in that it is not encumbered by the limitations concerning input amplitude and resolution, respectively. Some researchers have found this method to be suitable for systems with nonlinear damping characteristics (e.g. Jeary, 1992). However, the number of segments needed in

the ensemble may be quite high in order to produce a repeatable signature. Therefore, a large data set is required.

The conclusion that the resulting signature is the free vibration decay of the system does provide reasonable damping estimates in many cases. However, it has been shown to be mathematically incorrect (Vandiver et al., 1982). Specifically, the requirement of a uniform value for the initial condition of each segment biases the expected value of the excitation, and the last term in Eq. 14 is not necessarily zero in the average.

The solution to the equation of motion is given by:

$$x_T(t)x_o e^{-xw_n t}\left[\cos w_d t + \frac{w_n}{w_d}\sin w_d t\right] + \frac{\dot{x}_o}{w_d}e^{-xw_n t}\sin w_d t + \int_0^t h(t-t)\,f(t)\,dt \quad (16)$$

where $w_n = \sqrt{k/m}$; $w_d = w_n\sqrt{1-x^2}$; x_o and $\dot{x}_o$ are the displacement and velocity initial conditions; and *h (t)* is the system impulse response function.

The random decrement signature is the expected value of Eq. 17 conditioned by the initial values of each segment in the average, as in the following:

$$E[x_T \mid x_o, \dot{x}_o] = x_o e^{-xw_n t}\left(\cos w_d t + \frac{w_n}{w_d}\sin w_d t\right) + E\left[\frac{\dot{x}_o}{w_d}e^{-xw_n t}\sin w_d t\right] + \int_0^t h(t-t)E[f(t) \mid x_o, \dot{x}_o]dt \quad (17)$$

The first term on the right hand side is not affected by the expected value operator, and gives the free vibration response to an initial displacement. The magnitude of the second term on the right hand side is the same with an alternating sign over an even number of samples, which averages to zero. According to the intuitive theory, the expectation in the third right hand term vanishes since *f(t)* is a random zero mean process. However, since it is conditioned by the requirement of x_o and $\dot{x}_o$, it is not generally zero. Therefore, the intuitive interpretation of the random decrement signature as the free vibration response is not correct (Vandiver et al., 1982).

For the case where the excitation is stationary, Gaussian white noise, the autocorrelation of the response of a SDOF system is proportional to its free vibration response. For most applications, the random decrement scheme is applied to narrow-banded systems with relatively wide-banded excitation (e.g., building response to the buffeting effects of wind). For such cases, a white noise approximation is acceptable, and the intuitive explanation is appropriate, though not rigorously correct.

The resultant signature for a linear system under Gaussian stationary input is proportional to the autocorrelation of the system response, and is expressed as follows (Vandiver et al., 1982):

$$h(t) = E[x_T(t) \mid x_o, \dot{x}_o] = \frac{R_x(t)}{R_x(0)} x_o, \tag{18}$$

with a variance of

$$Var[h(t)] = \frac{1}{N} R_x(0) \left(1 - \frac{h^2(t)}{x^2{}_o} \right). \tag{19}$$

It is seen from Eqs. 18 and 19 that the variance is independent of the threshold level since it is assumed that there is no noise in the measured signal. If noise exists, the variance should increase with decreasing threshold levels.

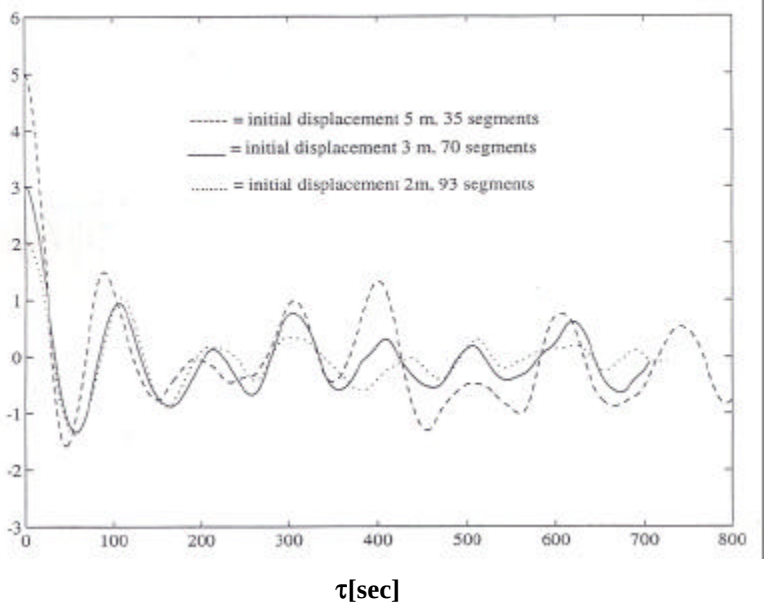

Figure 3: RDS of low frequency response of offshore platform *(taken from Kareem and Gurley, 1995*).

Several examples of the application of the RDT are now shown. The data set for the first two examples is the response of a model TLP subjected to wind and wave loads, and has a bimodal spectrum. The response of systems with more than one well-separated mode must be bandpass filtered about the desired mode in order to apply the random decrement method.

First, the low frequency mode is analyzed by low-pass filtering the data. The lengths of the data records proved to be too short to generate a repeatable signature. That is, the signature should give the same damping estimate regardless of the user-selected constant value at which segments are initiated. Figure 3 shows several random decrement signatures for the same system response. The signatures vary drastically from case to case, and a consistent damping estimate cannot be made among them. Notice also that the signatures do not resemble a free vibration decay signal.

The recommended number of segments is 400 to 500 according to some researchers (Yang et al., 1983), while others recommend at least 2000 (Tamura et al., 1992). The above records contain at most 6000 data points. For the low frequency mode, this included about 50 complete cycles. Each cycle can produce two segments for the ensemble average. However, 100 segments are not enough to sufficiently average out the random components of the response. In addition, the low frequency response is nonlinear, which violates the assumption of superposition of the response components.

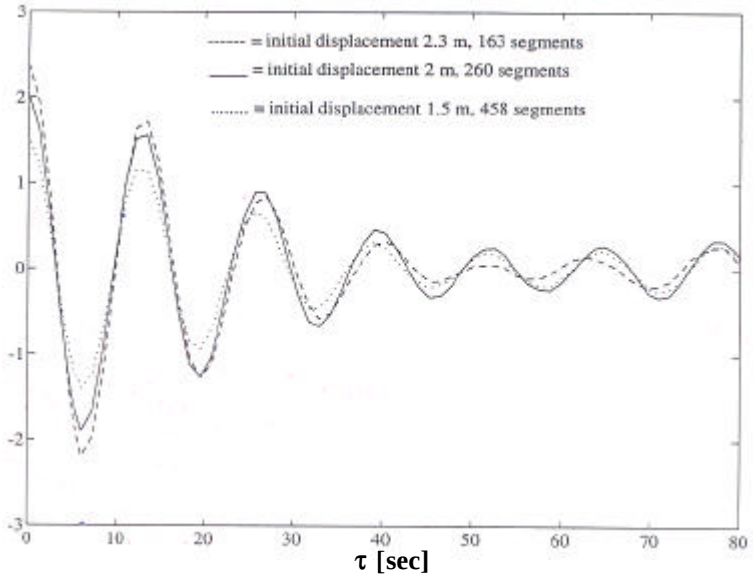

Figure 4: RDS for higher frequency response of offshore platform to wave field *(taken from Kareem and Gurley, 1995).*

The response of the platform also has a mode corresponding to the natural frequency of the incoming wave field. At the wave frequency, many more cycles are present in the recorded data than for the low frequency oscillation. This allows for more segments to be averaged when acquiring a random decrement signature. Figure 4 shows the random decrement signature for this higher frequency linear response to the wave field. The number of segments ranges from 163 to 458. These signatures are much more consistent with each other and more closely resemble a free vibration decay signature. The response at the wave frequency is linearly related to the input wave elevation, which corresponds to the assumption of superimposed responses. This signature may be used to estimate damping at this mode, but there is no exact value of damping to compare with this estimate.

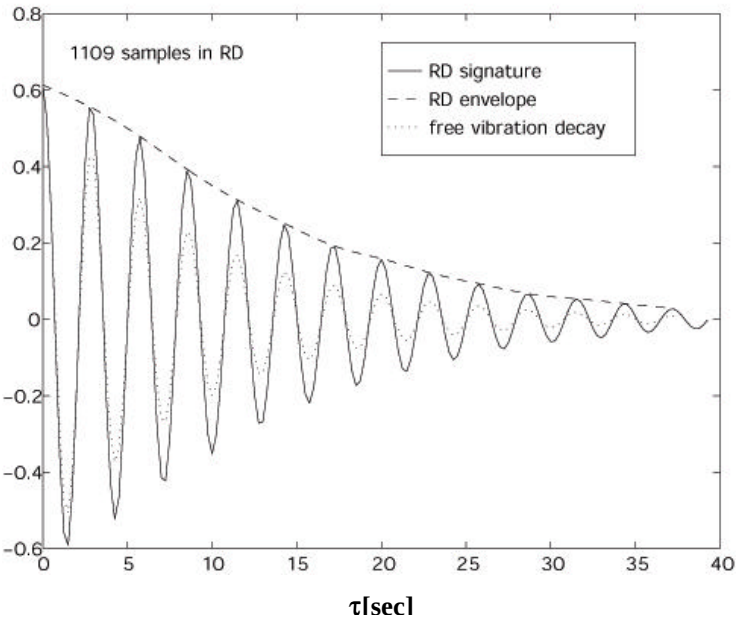

Figure 5: RDS and free vibration decay for linear oscillator excited by colored noise *(taken from Kareem and Gurley, 1995).*

In order to evaluate the applicability of the random decrement method to the above example, the response of a linear oscillator with a natural undamped frequency of 0.35 Hz and known damping to a wave train is numerically simulated at a sampling rate of 4 Hz. The RDS is then used to estimate the known damping value. A JONSWAP sea spectrum is applied to produce a linear wave train from standard frequency domain simulation techniques. The sea state used is fairly wide-banded, with a peakedness parameter of 1.0, and the system frequency is set at the peak of the input spectrum in order to better facilitate the white noise approximation. Figure 5 shows the random decrement signature of the oscillator response using 1109 overlapping segments with an initial displacement at each segment of 0.6. The known damping is 5% of critical, while the damping estimates from the signature using the logarithmic decrement and

half amplitude methods are 2.9% and 3.1%, respectively. Several threshold values were selected as initial displacement conditions in different runs, resulting in a consistent underestimation of the damping that ranged from 15% to 40%. Figure 5 also shows the actual free vibration response of the oscillator with an initial displacement equal to the corresponding threshold value. It is clear that the random decrement signature does not decay as quickly as the corresponding free vibration response.

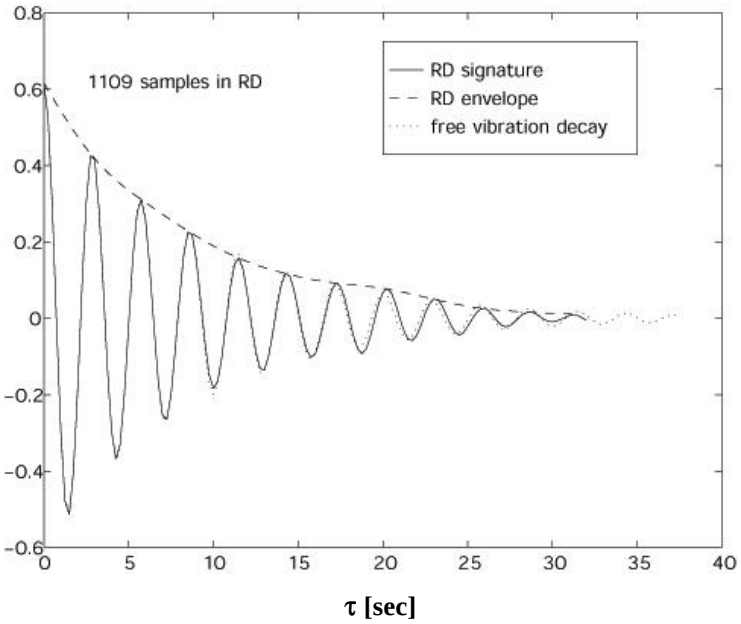

Figure 6: RDS and free vibration decay for linear oscillator excited by white noise *(taken from Kareem and Gurley, 1995).*

The same oscillator is subjected to white noise excitation with the same energy level as that of the above wave train in the range of the system's natural frequency. The resulting signature from 1109 overlapping segments with a 0.6 threshold value and the corresponding actual free vibration decay is shown in Figure 6. The estimated damping values are 5.3% and 4.9% for the logarithmic decrement and half amplitude methods, respectively. The damping estimates and the results in Figure 6, in comparison with those in Figure 5, demonstrate the importance of applying a white noise or wide banded input process in order to validate the application of the random decrement method.

The effects of violating the linear system assumption are investigated by replacing the linear oscillator with a nonlinear softening oscillator. This system is subjected to the same white noise input as the previous example. Figure 7 shows the resulting random decrement signature and free decay of the nonlinear oscillator using 1109 segments as before. The damping estimates are 5.5% and 5.2% for the logarithmic and half amplitude methods, respectively. It is noted that the frequency of the signature departs from that of the free decay as the amplitude decreases in the record, as a result of the system nonlinearity. This will affect the damping estimate depending on the particular cycles used for the damping estimation techniques. Here, they are the same as in the previous examples for consistency. The estimates are comparable to those of the linear system. However, they are not robust with respect to the selected threshold value and selected cycles for the applied techniques as they were for the linear system. Varying the threshold value from 0.3 to 0.8 for the linear system provides averaged damping estimates from the two methods in the range of 4.5% to 5.2%. For the nonlinear system, the estimates range from 4.4% to 5.8% and show a wide degree of scatter. This is because the dynamics of the non-linear system are amplitude-dependent, in contrast to the linear system.

The applicability of the RDT for estimating nonlinear systems, which manifested amplitude-dependent damping and natural frequency, was also investigated by Tamura and Suganuma (1996).

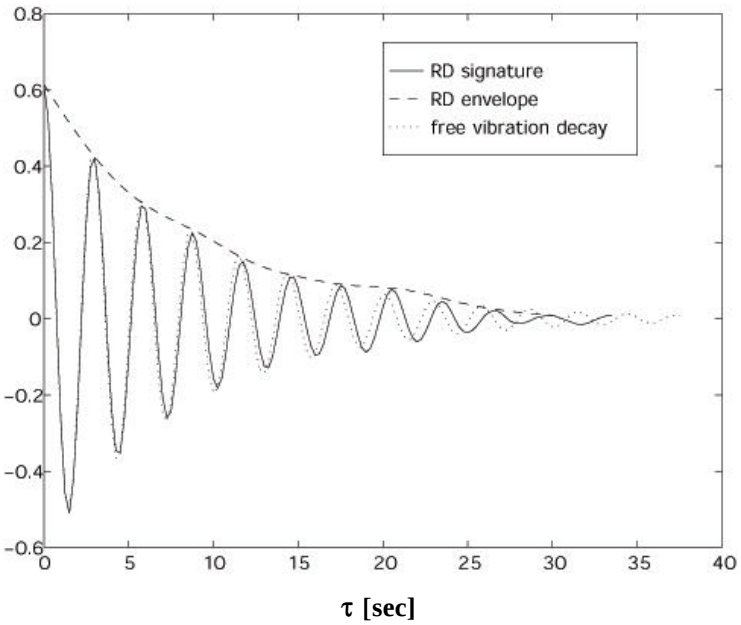

Figure 7: RDS and free-vibration decay of non-linear oscillator under white noise *(taken from Kareem and Gurley, 1995).*

Their findings illustrated that the quality of estimates in such non-linear systems depends upon the number of cycles considered in the estimate. By treating the non-linear system as locally linear at the triggering condition, the RDS is consistent with the free-vibration curve of the linear system for the level of damping and natural frequency associated with the amplitude level specified by the triggering condition. In this first cycle, as Figure 7 illustrates, the comparisons are good, and thus the use of RDT for these types of systems should restrict amplitude-referenced frequency and damping estimates to the values obtained from the first cycle of oscillation, where the system is locally linear.

The technique is next compared to the spectral damping estimation approach using the half-power bandwidth method. The response record of the linear oscillator subjected to white noise is segmented into 64 segments of 512 points each. These segments are windowed and the power spectral density is estimated using standard FFT methods. The half-power bandwidth method estimates the damping to be 3.8%, an underestimation of 24%. A longer data record may provide better estimates by adding resolution to the spectrum, but the random decrement method closely predicts damping with the current record length, as demonstrated above.

This method is well suited to the response of structures under buffeting wind loading, where the spectrum of the input process is wide-banded. However, wind forces that are the result of vortex shedding are narrow-banded in nature, leading to the same difficulties experienced in the above colored noise example.

2.3.4 Examples Using Extended Kalman Filtering

While the Kalman Filter had been used widely in linear system theory as a state observer, by augmenting the state vector, this approach may be extended to system identification through the Extended Kalman Filter. In essence, the concept is a form of sequential least square estimation adapted to the problem of parameter estimation for systems with measured input. However, while the typical sequential regression algorithm can only be used in linear and nonlinear elastic systems, the Kalman filter bears more flexibility in its extension to nonlinear systems, estimating the system parameters from relatively short observation records for multi-degree-of-freedom (MDOF) nonlinear systems (Yun & Shinozuka 1980). Examples employing equivalent linearization include Hoyshiya & Saito (1984) and Loh & Tsaur's (1988) applications of the Extended Kalman Filter to bilinear hysteretic systems. As a result, the Extended Kalman Filtering process is especially

attractive for system identification using earthquake induced vibrations, in which case the ground acceleration is readily available as input into the system.

The Kalman Filtering Algorithm, starting from an initial guess, recursively updates an extended state space representation as new observations are made available. Although the Extended Kalman Filter has been applied to MDOF nonlinear systems, its development herein is illustrated using a simplified single-degree-of-freedom (SDOF) linear oscillator. Readers are encouraged to consult the references provided for additional information on MDOF and nonlinear applications.

Consider the observed displacements of a SDOF system excited by input ground acceleration, a_g, described by the following equation of motion:

$$m\ddot{x} + c\dot{x} + kx = -ma_g \tag{20}$$

Accordingly, a discrete time state space representation of this system is given by:

$$\begin{aligned}
&\dot{\mathbf{x}}(i) = \mathbf{A}(i)\mathbf{x}(i) + \mathbf{B}(i)a_g(i) \\
&\mathbf{y}(i) = \mathbf{C}(i)\mathbf{x}(i) + \mathbf{D}(i)a_g(i), \quad \mathbf{x}(i) = \begin{bmatrix} \mathbf{x}(i) \\ \dot{\mathbf{x}}(i) \end{bmatrix} \\
&\mathbf{A}(i) = \begin{bmatrix} 0 & m^{-1} \\ -m^{-1}k(i) & -m^{-1}c(i) \end{bmatrix}, \quad \mathbf{B} = \begin{bmatrix} 0 \\ -1 \end{bmatrix}, \quad \mathbf{C} = \begin{bmatrix} 1 & 0 \end{bmatrix}, \qquad \mathbf{D} = [0]
\end{aligned} \tag{21}$$

In this general framework, stiffness, *k(i)* and damping *c(i)* for the system may vary at each time step *i*. For the system identification problem, specific components of the ***A*** matrix are unknown, specifically the stiffness, *k*, and damping, *c*, properties. (Although the mass of the structure is typically known, the augmented state vector in the Extended Kalman Filtering process may also be recast to include mass as an unknown quantity (Hoshiya and Saito 1984).) In this case, the states are extended to include the unknown quantities:

$$\mathbf{x}(i) = \begin{bmatrix} \mathbf{x}_s(i) \\ \mathbf{x}_p(i) \end{bmatrix} = \begin{bmatrix} x(i) \\ \dot{x}(i) \\ k(i) \\ c(i) \end{bmatrix} = \begin{bmatrix} x_1(i) \\ x_2(i) \\ x_3(i) \\ x_4(i) \end{bmatrix} \tag{22}$$

where $\boldsymbol{x_s}$ indicates the states to be identified and $\boldsymbol{x_p}$ indicates the parameters to be identified. Thus, in place of the matrix ***A***, the differential equation of motion is described as a function, ***f (x)***, of the augmented states:

$$\dot{\mathbf{x}}(\mathbf{i}) = \mathbf{f}(\mathbf{x}(\mathbf{i})) = \begin{bmatrix} x_2(i) \\ -\frac{x_3(i)x_1(i)}{m} - \frac{x_4(i)x_2(i)}{m} - a_g(i) \\ 0 \\ 0 \end{bmatrix} \tag{23}$$

$$y(i) = \mathbf{H}(\mathbf{x}(\mathbf{i})) + \mathbf{v}(\mathbf{i}) = \begin{bmatrix} x(i) & 0 & 0 & 0 \end{bmatrix} + v(i)$$

where v is assumed to be zero mean, Gaussian white noise with a covariance matrix, $R(i)$ at all discrete times, t_i.

Since the initial conditions of the system are uncertain, the initial states may be described as a stochastic quantity, assuming that the initial state is taken from a vector of Gaussian random variables, $\mathbf{x}(0) \sim N(\mathbf{x}(0), \mathbf{P}(0))$.

The Extended Kalman Filtering analysis begins with choice of the initial error covariance matrix and initial state estimate, ***P(0)*** and ***x(0)***, respectively, to begin the iterative process. The state and error matrix are then propagated from the previous time step to the current time using the following equation:

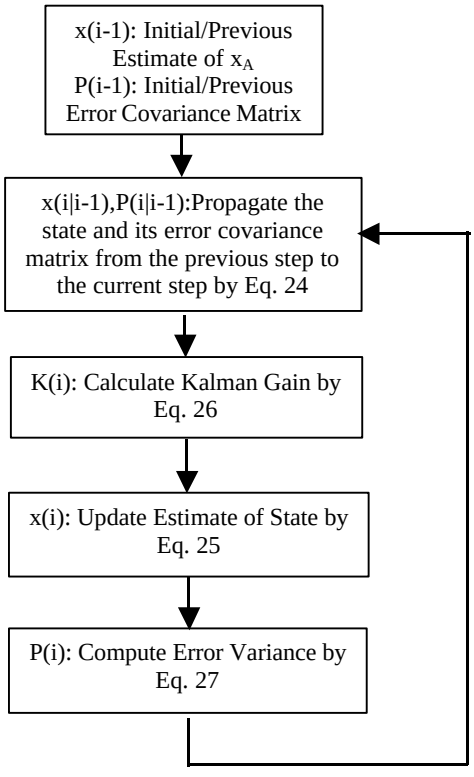

Figure 8: Overview of the Extended Kalman Filter iterative scheme.

$$\mathbf{x}(i \mid i-1) = \ddot{\mathbf{O}}(i, i-1)\mathbf{x}(i-1)$$
$$\mathbf{P}(i \mid i-1) = \ddot{\mathbf{O}}(i, i-1)\mathbf{P}(i-1)\ddot{\mathbf{O}}^T(i, i-1) \tag{24}$$

where ***F(i,i-1)*** is the state-transition matrix. Based on this information, an estimate of the state vector at the i^{th} step can be updated by:

$$\mathbf{x}(i) = \mathbf{x}(i \mid i-1) + \mathbf{K}(i)[y(i) - \mathbf{H}(i)\mathbf{X}(i \mid i-1)] \tag{25}$$

Where ***K(i)*** is the Kalman Gain given by

$$\mathbf{K}(i) = \mathbf{P}(i \mid i-1)\mathbf{H}^T(i)[\mathbf{H}(i)\mathbf{P}(i \mid i-1)\mathbf{H}^T(i) + R(i)]^{-1} \tag{26}$$

The error variance may then be calculated by

$$\mathbf{P}(i) = \mathbf{P}(i \mid i-1) - \mathbf{K}(i)\mathbf{H}(i)\mathbf{P}(i \mid i-1) \tag{27}$$

The state-transition matrix is typically determined by a first order Taylor Series expansion:

$$\ddot{\mathbf{O}}(i, i-1) = \mathbf{I} + \Delta t\mathbf{F}(i) \tag{28}$$

where ***I*** is the identity matrix, *Dt* is the time step between observations and ***F (i),*** the gradient of ***f****(x),* is defined by

$$\mathbf{F}(i) = \left[\frac{\partial \mathbf{f}(x)}{\partial x_j} \right]_{x(i)} \tag{29}$$

evaluated at ***x(i)***.

Due to this approximation, the accuracy of the approach will depend upon the size of the time step employed. Thus, the Extended Kalman Filter typically requires a higher sampling rate than traditional system identification approaches (Ghanem & Shinozuka 1995).

Once the estimate of the state and its error covariance matrix is determined, the process is repeated using these most current estimates, as shown in Figure 8, over the entire course of the observed response.

While the Extended Kalman Filter has many attractive features, there have been concerns regarding its stability, the convergence of estimated parameters to exact ones, and the sensitivity of convergence and accuracy to the initial conditions. In fact, the final values themselves are very much dependent on this initial guess, as estimates may indeed be convergent, but to erroneous results. Through the use of rational orthogonal polynomial curve fits, authors have been able to estimate reliable first guesses into the Extended Kalman Filter, improving its convergence and accuracy (Shinozuka & Ghanem 1995). The authors further noted the rapid deterioration of the linear acceleration approximation for the state-transition matrix in the presence of low sampling rates, prohibiting convergence in some multi-degree-of-freedom analyses. Considering particular challenges with white-noise-excited structures, the authors recommended a time step of one-twentieth of the lowest period of the structure for accurate results.

With the availability of only finite duration observations, particularly common in applications to earthquake engineering where records last a number of seconds, arbitrarily assigned initial conditions may not produce stable solutions convergent to the actual system parameters. To remedy some of the concerns surrounding the accuracy of the Extended Kalman Filter, Hoshiya and Saito (1984) proposed a weighted global iteration scheme to obtain stable solutions with fast convergence. The Extended Kalman Filter with Weighted Global Iteration (KF-WGI) employs a global iteration scheme coupled with the use of an objective function, improving the applicability of this system identification approach for MDOF linear systems, bilinear systems and hysteretic systems.

Essentially, the Kalman Filtering Algorithm as outlined in Figure 8 is executed over the entire duration of observed data, *y (i).. i=1:N*, based upon the initial guesses for the states and error covariance matrix. Then, the results of the first filtering step, estimates of the states ***x*** *(N)* and error matrix ***P*** *(N)* at the final observation time are fed into the next phase of the iterative scheme as a new initial "guess" along with a calculated objective function *q*, as shown in Figure 9. The error covariances associated with the parameters to be identified are weighted by the constant *W* and the Kalman Filtering Scheme is repeated until the objective function is minimized. The iterative scheme helps to improve the accuracy of the approach by constantly refining the quality of the initial guesses into the Extended Kalman Filtering Algorithm, while providing an objective function to gauge the accuracy of the estimated states. Such a reliability estimate is crucial, as the Extended Kalman Filter may converge to erroneous values.

Hoshiya and Saito (1984) had noted that while a large initial covariance is favorable in order to accelerate the Extended Kalman filter's convergence, stability may be somewhat affected. By introducing the weighted covariance matrix, the trade off between these two effects can be maximized to some extent, while the global iteration scheme helps to improve the performance of the algorithm even with poor initial estimates of the states.

While the Kalman Filtering technique has been applied extensively for parameter identification, authors have noted difficulties associated with the scheme. Shinozuka and Ghanem (1995), among others, have observed the sensitivity of the filtering scheme to the time step, as this greatly impacts the ability of the linear acceleration method to approximate the state-transition matrix, as shown in Eq. 28. These challenges are of course in addition to the sensitivity of the scheme on the initial guesses for the unknown parameters and the associated covariance matrix, though the implementation of the weighted global iteration scheme has aided in this matter.

As mentioned previously, KF-WGI may also be modified to account for unknown mass, as shown by Hoshiya & Saito (1984). The algorithm has more difficulty estimating the parameters of the system in this case, with no clear convergence in the global iteration scheme; however, the use of the objective function did help the authors identify the best estimate of the system parameters within about 10%. The poor performance in this case may also have been attributed to the fact that response quantities for the three-degree-of-freedom system were measured at only one location, as MDOF identification by this approach is more accurate when measurements at all degrees-of-freedom are available. These observability issues later prohibited parameter estimates in the same study for a MDOF, nonlinear system when the output was measured at only one degree-of-freedom. These observability problems were also encountered by Shinozuka & Ghanem (1995), particularly when white noise excitations were used as system inputs.

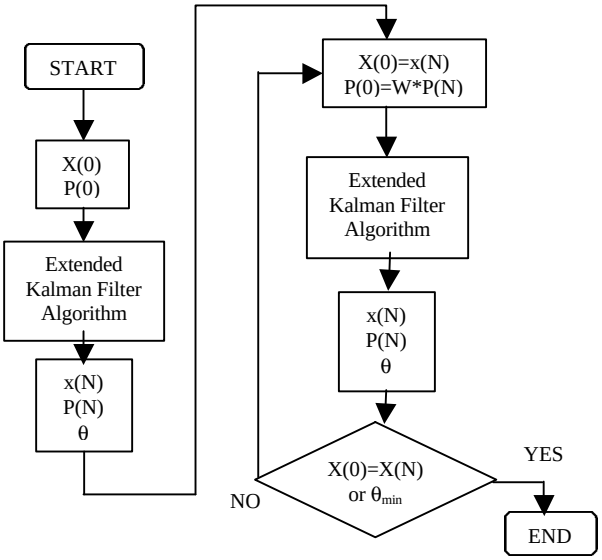

Figure 9: Weighted global iteration procedure *(adapted from Hoshiya & Saito 1984).*

While the KF-WGI algorithm has been able to overcome some of the convergence issues raised herein, diminishing the effects of poor initial guesses, the appropriate selection of sampling rate is critical, particularly in the case of lightly damped structures. As true of most system identification approaches, damping is more difficult to estimate than natural frequency, as it plays less of a role in the overall structural response. The following example explores the ability of KF-WGI to accurately estimate the parameters of a lightly damped SDOF oscillator.

The oscillator was excited by the El Centro Earthquake record, with observations only moderately corrupted by white noise of 1% the RMS displacement response of oscillator. To illustrate the ability of KF-WGI to overcome poor initial guesses, the initial estimate of the extended state space

vector was chosen as $\mathbf{x}(0) = \begin{bmatrix} x(0) \\ \dot{x}(0) \\ k(0) \\ c(0) \end{bmatrix} = \begin{bmatrix} 0 \\ 0 \\ 1 \\ 1 \end{bmatrix}$ and the initial error covariance matrix, ***P(0)***, was defined as the identity matrix. Estimates of the structural parameters were determined using 30 seconds of data, sampled at 0.02 Hz, and the global iteration weight was chosen to be 1000. Some discussion of the selection of weights is provided in Hoshiya and Saito (1984).

Table 1: Performance of KF-WGI for SDOF Parameter Identification.

	Actual		**Estimate Errors**	
	f_n	**ξ**	**f_n**	**ξ**
Case 1	5 Hz	1%	0.7381%	0.8634%
Case 2	3 Hz	1%	0.0571%	0.9773%
Case 3	0.5 Hz	1%	2.9735%	8.3922%
Case 4	0.5 Hz	0.5%	2.5141%	13.88%

Table 1 summarizes the results of four cases with varying natural frequency, f_n, and critical damping ratio, x. By fixing the sampling rate, the four cases illustrate the performance of KF-WGI for lightly damped, low frequency systems. While the estimates are within 1% error for the first two cases, decreasing the system frequency leads to less accurate estimates of damping and even frequency. By decreasing the damping of the system, the ability of KF-WGI to accurately estimate the system's parameters diminishes, illustrating the challenges associated with estimating damping in lightly damped systems.

Figure 10 illustrates the benefits of the Global Weighted Iteration scheme. Note that in all cases, the initial guesses were especially poor, with the results of the first weighted global iteration straying significantly from the actual parameter values. The use of weighting leads to rapid convergence within two global iterations, illustrating the improvement in estimates as the result of just a few global iterations.

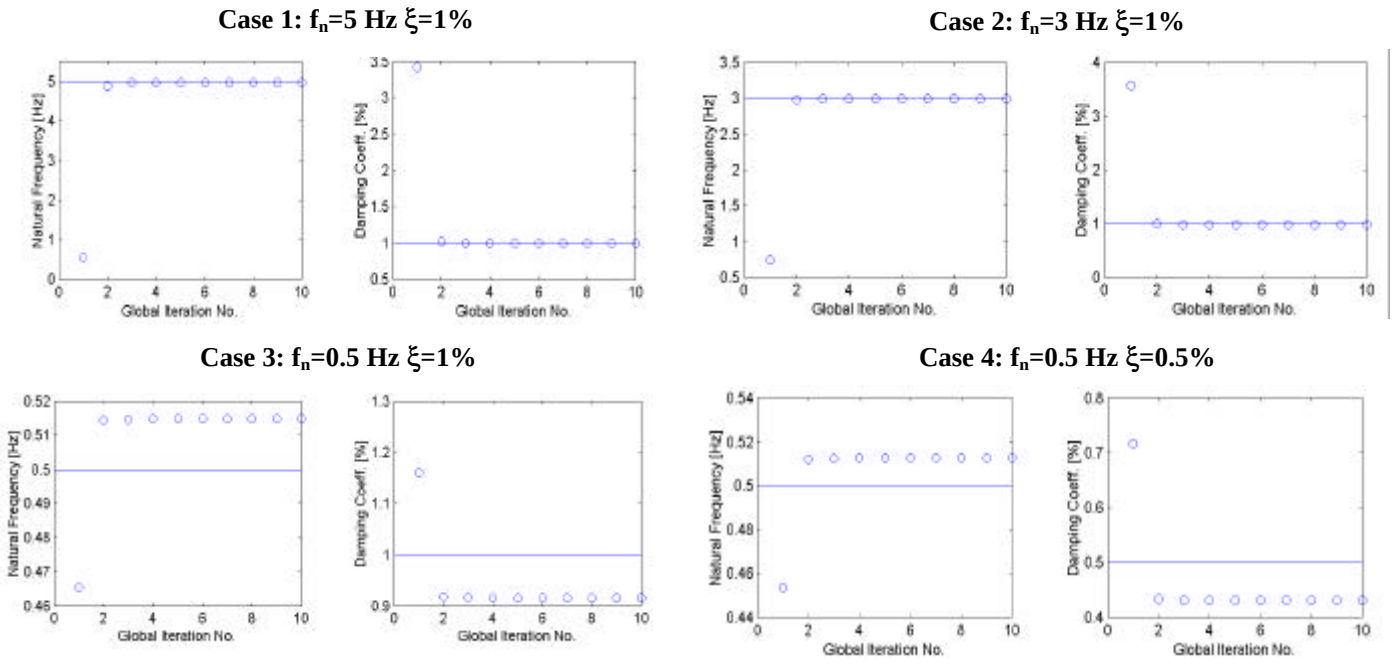

Figure 10: Variation of Extended Kalman Filter estimates with number of global iterations, 4 cases considered. (o = KF-WGI estimate; __ = actual parameter value)

2.4 Concluding Remarks

In this section, structural and aerodynamic damping mechanisms were discussed separately, and recent advances in each were summarized. The estimation of damping using the Random Decrement Technique was presented in detail. Examples demonstrated the utility of this method compared to spectral methods that are subject to resolution restrictions. In addition, this section also discussed the limitations of the RDT in that its application requires nearly white noise input and a nearly linear system. Kalman Filtering approaches were presented as an alternative approach. KF-WGI is attractive, but the requirement of exact inputs prohibits its direct use in wind-induced vibration response. Since the present state-of-the-art in the design of tall buildings does not permit accurate damping estimates until the building construction is complete, the methodologies illustrated here offer possible tools for the estimation of building response with uncertain damping.

3 Damping Properties of Buildings: Databases

Structural damping is the most important, yet most uncertain parameter affecting the response of buildings and structures (Kareem, 1988). As discussed in the previous section, uncertainty in the damping parameter significantly reduces the reliability of structural design for dynamic effects. Accurate determination of structural damping is very important not only for evaluating the structural response, but also for designing auxiliary damping devices to be installed in buildings and structures. As stated above, there is no widely accepted method available for estimating damping ratios of structures prior to construction. This section discusses a high-quality, full-scale

damping database proposed in Tamura et al. (1996) for buildings and structures to establish methods for assessing damping ratios at the design stage.

3.1 Necessity of a Damping Database

An accurate predictive model for damping is becoming increasingly necessary to aid designers in estimating damping ratios based on building properties. This predictor should be able to reflect effects such as structural materials, types or shapes of frames, types and amounts of interior and exterior finishing, types of foundations and soils, and so on. The effect of amplitude also has to be included, and different values should be assessed for the serviceability limit state design and the ultimate limit state design. Clearly, reliable full-scale damping data of buildings of various types and conditions must be accumulated. There has been no such high-quality database with enough data from enough building types in which the quality of the data has been strictly assessed from various viewpoints. There is an urgent need for the collection and labeling of such a database.

It is well known that nonlinear characteristics appear in both natural frequencies and damping ratios. The damping of tall steel buildings is thought to be dominated by friction between frames, secondary members and claddings (Jeary, 1986; Davenport and Hill-Carroll, 1986). It is clear that the damping mechanism and the overall stiffness of a structure are different aspects of the same physical mechanism. Therefore, it is also important for the damping database to include information on natural frequencies.

3.2 Quality of the Damping Data

Measured damping ratios vary according to a number of factors including, vibration amplitude, structural materials, soil and foundation types, architectural finishing types, joint types and the number of non-structural members. Furthermore, due to the nonlinearity of the dynamic characteristics of buildings and the nonstationarity of excitations, the estimated damping ratios tend to differ depending upon the evaluation technique. However, vibration measuring techniques and data processing have significantly improved with the development of microprocessor-based devices and software. In addition, the RDT discussed previously, which is a fairly nonstationarity-tolerant damping evaluation method, has been widely used (Tamura et al., 1993).

In Japan, the Committee on Damping Evaluation was organized in 1992 in the Building Center of Japan. Its work was taken over by a committee of the same name that was organized in the Architectural Institute of Japan in 1993. As a result of this committee's activities and promotion, research on structural damping has greatly increased in Japan recently. Structural damping has been evaluated very carefully, and the accuracy of the published data has improved. Many Japanese buildings are currently equipped with vibration monitoring for active or passive damping devices or for endorsement of design assumptions. Clearly, the dynamic characteristics of these buildings under various types of excitations would provide valuable insights.

More than twenty committee members representing research institutes, structural design offices, and construction companies offered their own recent reliable data that satisfied required conditions in a specified format. Additional damping data have been collected from many journals and

proceedings published after 1970. Basic analyses of the collected damping data were made by Suda et al. (1995).

3.3 Reliability of Japanese Damping Database

Questionnaire studies were mailed to literature authors, designers, and building owners by the AIJ Committee to obtain information regarding measurement and evaluation techniques and vibration amplitudes. Data whose reliability could not be confirmed were excluded. The data whose amplitudes were not clarified or could not be assumed from the measuring methods were also excluded. Consequently, many original non-published data were collected and additional information was added to the published data by the committee. The damping data collected in the database are believed to be highly reliable. However, the stationarity of a record of wind-induced responses should be guaranteed when a spectrum-based technique is applied to evaluate damping from the response record (Jeary, 1992). However, the stationarity of the record was never exactly checked in the measurement. Therefore, the stationarity of the data in the database should be considered as unknown. As a result, the final judgment regarding the reliability of each data set would be left to the user of the database. The inclusion or exclusion of the data in analysis can be decided by the user depending upon various information contained in the database.

Additional questionnaire studies were conducted of all the collected unpublished data to obtain approval for worldwide distribution. Only the approved data are contained in the database. The dynamic properties of 268 buildings and structures had been collected by the AIJ Damping Committee as of October, 1996. Information contained in the database is summarized in Table 2 (Tamura 1997).

Table 2. Japanese Damping Database as of October 1996.

<table>
<tr><td colspan="5">Number of Buildings and Structures</td></tr>
<tr><td colspan="5">268</td></tr>
<tr><td>Steel Buildings</td><td>Reinforced Concrete Buildings</td><td colspan="2">Steel Encased Reinforced Concrete Buildings</td><td>Tower-Like Structures</td></tr>
<tr><td>135</td><td>28</td><td colspan="2">46</td><td>59</td></tr>
<tr><td colspan="5">Contained Information</td></tr>
<tr><td rowspan="5">Modeling Information</td><td>Building ID Number</td><td>Location</td><td colspan="2">Time of Completion</td></tr>
<tr><td>Building Usage (Purpose)</td><td>Shape</td><td colspan="2">Height</td></tr>
<tr><td>Dimensions</td><td>Number of Stories</td><td colspan="2">Structural Type</td></tr>
<tr><td>Cladding Type</td><td>Foundation Type</td><td colspan="2">Depth of Embedment</td></tr>
<tr><td>Length of Piles</td><td>Soil Conditions</td><td colspan="2">Reference</td></tr>
<tr><td rowspan="3">Dynamic Properties</td><td>Dynamic Ratio
• Longitudinal (up to the 6th mode)
• Transverse
• Rotational</td><td>Natural Frequency
• Longitudinal (up to the 6th mode)
• Transverse
• Rotational</td><td colspan="2">Time of Measurement</td></tr>
<tr><td>Excitation Type</td><td>Experimental Method</td><td colspan="2">Measurement Method</td></tr>
<tr><td>Evaluation Technique</td><td>Amplitude</td><td colspan="2"></td></tr>
</table>

Percentages of the various experimental and damping evaluation methods contained in the database are tabulated in Tables 3 and 4 (Tamura 1997).

Table 3. Experimental Methods.

Excitation Type		Vibrators and Vibration Sources	
Forced Oscillation	25%	Mechanical Shakers	94%
		Active Dampers	6%
Free Oscillation	30%	Mechanical Shakers	14%
		Active Dampers	2%
		Man Power	58%
		Pull and Release	10%
		Pendulums	6%
		Others	10%
Natural Excitations	45%	Microtremor	60%
		Wind-Induced Response	31%
		Earthquake Response	9%

Table 4. Damping Evaluation Methods

Excitation Type	Evaluation	
Forced Oscillation	Resonance Curve: $1/2^{1/2}$	61%
	Resonance Curve: Curve Fitting	39%
Free Oscillation	Logarithmic Decrement	100%
Natural Excitations	Autocorrelation Function	15%
	Random Decrement Technique	39%
	Half Power Spectrum	20%
	Curve Fitting Spectrum	17%
	Transfer Function	5%
	System Identification	1%
	Others	3%

3.4 Concluding Remarks

This section discussed a reliable database of damping values for many different types of structures under various different loading and excitation conditions, providing the data to possibly develop a more accurate damping predictor that will ensure more realistic dynamic structural design. Due to the high cost and scarcity of full-scale investigations, this database is accessible to any researcher or practitioner interested in the damping of buildings and structures. Still, there is a pressing need to extend this database for international collaboration to exchange and collect reliable damping data.

4 Damping Systems and Their Performance

As discussed above, wind-induced oscillations of tall buildings may not be significant enough to cause structural damage. However, in some cases, such motion may result in discomfort to the

building's occupants. Such wind-induced responses of tall buildings under design can be controlled by global design modifications (Kareem et al. 1999). These modifications can be placed into the following three categories: modification of the structural system, modification of the structure's aerodynamic properties, and the provision of auxiliary damping in an existing structure. In the following section, these methods for increasing the damping of a structure are discussed in detail.

An efficient structural system can provide the most effective means for controlling structural responses. Other options may include altering the mode shapes to benefit from increased mass and shifting of the major frequency axes from the main axes of the building shape. Appropriate selection of a building shape that offers minimum wind-induced load effects can control building motion right at the source. Additionally, changing the building's shape or cross-sectional dimensions near the top helps to vitiate the effects of the organized vortical flow structure that is responsible for coherent loading. Architectural modifications such as corner geometry, fins, setbacks, tapers, buttresses, and openings through the upper portion of the building can help to reduce the wind loading and associated building motions. Examples of these architectural modifications are very prevalent in new tall buildings, especially in Japan.

4.1 Auxiliary Damping Devices

As discussed in Section 2.0, the estimates of damping in structural systems have intrinsic variability that makes the assessment of the serviceability limit states more uncertain (Kareem and Gurley, 1995). Such uncertainty can be overcome by introducing a known level of damping through an auxiliary source. By applying such an auxiliary damping device to a structure, the damping level of the structure increases, resulting in a reduction in the wind-induced motion. Auxiliary damping sources can be categorized into passive and active systems. Both passive and active systems may be further categorized based on their mechanism of energy dissipation, i.e., mass or inertial effects and direct energy absorption. Systems that rely on energy absorption devices with variable characteristics, such as the variable orifice or MR or ER dampers, are placed into the subcategory of semi-active systems. While complete details of these systems and their applications cannot be provided herein, readers are encouraged to consult Kareem et al. (1999) for further details.

4.2 Passive Systems

Passive systems impart indirect damping to a structure through modification of the structural characteristics. The most popular concept among passive systems is the damped secondary inertial system. Such systems include tuned mass dampers (TMDs) and tuned liquid dampers (TLDs), which include sloshing dampers (TSDs) and liquid column dampers (TLCDs) (McNamara, 1977; Kareem, 1983; Tamura et al., 1988; Sakai et al., 1989; Fujino et al., 1992). Like a TMD, the TSD and TLCD impart indirect damping to the system by modifying the frequency response of the system, thereby reducing the structural response.

A TMD typically consists of an inertial mass attached near the top of the building through a spring and damping mechanism. Viscous and visco-elastic dampers are typically used to provide the damping of the TMD system. The difficult logistics of moving a large mass have led to a number of innovative configurations. In these schemes, the damper mass can either move in the horizontal

or vertical plane. For the horizontal motion configuration, the damper mass is levitated in an oil bath and nitrogen gas springs are used to tune the damper frequency, i.e., it is placed on multi-stage rubber bearings. Several types of pendulum actions are used in the vertical plane motion of the damper mass. However, for structures with a long period, a several story high pendulum may be needed. This shortcoming is eliminated by employing a multi-stage pulley system or a multiple mass system. The indirect damping imparted by a TMD is determined by the size of the damper and the stroke distance (i.e., the travel distance of the mass). The damping is also dependent on the ratio of the damper mass to the effective mass of the building in the mode of interest, which is governed by economic considerations and the availability of space. It is typically in the range of one percent of the building mass in the fundamental mode.

The sloshing liquid absorbs structural energy and dissipates it by means of the viscous action of the liquid, wave breaking, screens, and baffles. Similarly, in a TLCD, an orifice or multiple orifices provide a source of energy dissipation in the oscillating liquid. Unlike a TMD, a TSD has an amplitude dependent transfer function that is further complicated by the nonlinearity of the sloshing process and wave breaking. The damping value of a TLCD is also sensitive to the level of excitation. Due to a lack of free surface, the system does not exhibit nonlinear behavior as in TSDs. The liquid dampers offer a more convenient utilization of space and weight when the building water supply tank can be used as a damper. Multiple damper configurations with slightly detuned systems have shown to be more effective than a single isolated damper. For the same total mass, the equivalent damping introduced to the system by multiple dampers is almost twice as much as that due to a single damper (Kline and Kareem, 1995). Furthermore, the optimal damping is also much lower than a single damper, which makes it more attractive for liquid dampers.

Other versions of liquid dampers exist, including inertial pump dampers, or configurations in which water in a compartmentalized tank is moved back and forth in the same way that dinghy sailors move their weight outboard to control heeling. By applying controlled air pressure to a TLCD configuration, systems can be tailored to offer more flexibility in the tuning frequency without changing the water column height.

The damping systems that involve direct dissipation of damping include viscoelastic dampers, friction, viscous, oil, lead, steel, joint, and impact-type dampers. The viscoelastic dampers are the most promising and have been installed in several buildings both in Japan and in the United States (Keel and Mahmoodi, 1986; Fujita, 1991; SEF, 1994).

TMDs have been in service for several years in the Citicorp Building in New York and in the John Hancock Building in Boston, where a pair of TMDs is used. Their performance in these structures has been satisfactory as reported in the literature. A TMD system is also planned for an air traffic control tower at Washington National Airport. In Australia, the Sydney Tower is equipped with two TMDs, and the 52-story Chifley Tower office building uses a pendulum type TMD. In Japan, there are several buildings and towers in which TMDs have been installed. These include the Chiba Port Tower, the Higashiyama Sky Tower, the Crystal Tower, Fukuoka Tower, Rokko Island P&G, Akita Tower, and the Nagasaki Huis Ten Bosch Domtoren. These systems vary in their configuration. Some have a mass on rollers with springs or supported on multiple rubber bearings, while others are of the pendulum type. Some of these are uni-directional, and some have bi-directional capabilities. Additional references concerning the details of these dampers and the

building or tower features are Fujita (1991), Izumi et al. (1993), and Sakamoto and Kobori (1996). The performance of most of these systems has been monitored by full-scale measurements. A summary of measurement results can be found in Tamura (1993).

Energy absorption systems such as viscoelastic dampers, viscous dampers, friction dampers, and dampers utilizing hysteretic behavior, including metallic systems such as steel, shape memory alloys, or lead dampers are used in buildings or other structures. In the United States, viscoelastic dampers (VEDs) have been used in the World Trade Center Towers in New York and in the Columbia Building in Seattle. In Japan, VEDs have been installed in the Shibaura Seavans Building and in the Chiba City Gymnasium. Frictional dampers are included in the Sonic City Office Building and the Asahi Beer Tower in Japan. Hysteretic metallic dampers made of lead come in different forms and have been installed in the Fujita Kogyo Building in Tokyo. The steel dampers are incorporated in Kajima Corporation's KI Building complex. Details of their performance can be found in Tamura (1993). There are several applications of a variety of damping systems in the United States for seismic protection (ATC, 1993; SEF, 1994; Seismic Design Symposium, 1995). Most of these devices can also be used to control wind-induced motion.

The TLDs are gaining in popularity in Japan. The Gold Tower is equipped with a rectangular liquid tank with nets, "Aqua Dampers," to enhance damping. A 27-meter-high office building has a U-tube type liquid damper with a pressurizing system that has a variable control on the frequency of the oscillation. The Tokyo International Airport Tower at Haneda utilizes TLDs with floating particles to enhance damping, due in part to surface tension. TLDs are also installed in the Narita and Nagasaki Airport Towers. The Shin-Yokohama Prince Hotel is equipped with shallow circular containers at the top floor of the hotel. Full-scale tests have shown that the system is effective in reducing the response and improving the serviceability, and also reduces in the range of 50-70 percent at wind speeds above 20 m/sec. Recently, U-shaped water tanks known as "Movics," have been installed to control bi-directional motion of Hotel Cosima in Tokyo, the Hyatt Hotel in Osaka, and the Ichida Building in Osaka (Shimizu and Teramura, 1994). The dampers have the flexibility of adjustment in their natural periods.

4.3 Active Systems

Active control devices reduce the structural response by means of an external energy source (Soong, 1990; Suhardjo et al., 1992). Structural motion can be controlled by an active mass damper (AMD) or an active bracing system (ABS). Other active configurations in practical use may be found in Fujita (1991). The AMDs are configured such that the active mass is either in a sliding or pendulum mode. In the case of a pendulum mode, multiple pendula can be used to account for long periods. The mass ratio in the case of active systems can be lower than their counterpart passive systems due to their improved efficiency, while the damper mass stroke is larger for heavier buildings and for buildings with a lower damper mass. For active systems with a lower secondary mass, more control force is required. The actuators used in active systems are hydraulic or use AC servomotor systems.

A hybrid system may be utilized to overcome the shortcomings of a passive system, e.g., its inability to respond to suddenly applied loads like earthquakes and weather fronts. In the case of a

TMD, the building may be equipped with a passive auxiliary mass damper system and a tertiary small mass connected to the secondary mass with a spring, damper, and actuator. The secondary system is set in motion by the active tertiary mass, and it is driven in the direction opposite to the TMD and magnifies the motion of the TMD, making it more effective. An example of such a system is known as "Duox," and has been installed in the Ando Nishikicho Building in Tokyo (Koshika et al., 1992).

In Japan, a tuned active damper has recently been installed in the Landmark Tower in Yokohama. The tuned system has a multiple-stepped pendulum and an AC servomotor is used for its control. The system is effective against low level vibrations, but works equally well to counteract more serious swaying caused by strong winds (Yamazaki et al., 1992). Similar systems are installed in the Mitsubishi Juko Yokohama Building and in the NTT CRED Motomachi Building. Alternatively, a roller pendulum and active structural response control produce a compact, lightweight, high-performance system. Such a device is installed in the Shinjuku Park Tower in Tokyo. This system has the flexibility of an adjustable damper period from 3.7 to 5.8 seconds, and three units are installed for serviceability enhancement. Other current applications of an AMD or a hybrid system include: the Kansai New International Airport Tower (two pendulum type AMDs); an experimental building of Shimizu Corporation (multi-stage rubber bearings supporting a bi-directional AMD); ORC Symbol Tower (passive in one direction and active in the other), C Office Building, ACT City (multi-stepped pendulum in one direction and passive damper in the other), and K Office Building (two AMDs, one for transverse and the other for torsional motion). In addition, two active gyro dampers are installed in a tower utilizing an actively controlled motor. It is interesting to note the choice of active in one direction and passive in the other in many applications in Japan. Also, some of the systems are active in a certain range of operation and passive beyond a pre-established limit.

4.4 Semi-Active Systems

A semi-active system may be utilized to overcome the shortcomings of a passive system such as a TLCD, which is rather slow in responding to sudden gust fronts. Also, the damping in a TLCD is dependent on the level of excitation. This feature renders the operation of TLCDs mainly at non-optimal values of damping. In order to improve the efficiency of the TLCD, the size of the orifice can be controlled by the feedback information on the level of liquid oscillation (Kareem, 1994). In another configuration, the liquid motion in a TLCD can be controlled by a feedback controller that initiates liquid motion over a finite "start-up" transient by the action of actively controlled pistons (Kareem, 1994). Once liquid motion has been established, the controller can be disengaged if desired. Other advantages of introducing active control may include flexibility in making adjustments in the natural frequency of the liquid oscillation by adjusting pressure over the water column as well as the potential for driving in some cases to enhance the efficiency of the passive TLCD system. Other semi-active systems like the variable orifice, ER and MR type dampers have recently been studied and have shown great potential (2IWSC, 1996).

4.5 Concluding Remarks

This section addressed a number of passive and active motion control devices for improving the performance of tall buildings under wind loads for human comfort considerations. Examples of

practical implementation of these devices in Australia, Canada, Japan and the United States were given. The section also highlighted prospects for the future by improvising passive systems utilizing a semi-active control mechanism to enhance their effectiveness.

5 Tailoring Damping in Structures: Design Issues

As discussed above, the addition of damping into structural systems is an efficient method for reducing the effects of dynamic loads. Over the past twenty-five years, the concept of a separate system to increase the damping in buildings has gained widespread acceptance. These systems, which were discussed in the previous section, have been introduced in large scale structures to mitigate the effects of frequent storms on occupant comfort. These systems can be thought of conceptually as simply increasing the "effective" damping of the structure.

5.1 General: Damping and Energy Dissipating Systems

In the design of tall buildings, wind engineers must assume a level of inherent damping in the structure in order to assess the habitability under frequent storms. The actual damping in buildings is difficult to measure and varies with response levels, the type of structural and cladding systems used, and the materials used for construction. The inherent damping in a structure cannot be determined with the same degree of accuracy as other dynamic characteristics such as the mass or period.

The amount of actual damping present in a structure has a significant effect on its dynamic response. Changes of assumed damping from 1% effective to 2% effective can reduce the RMS acceleration response of a tall building by as much as 20% to 30%. Because of this uncertainty associated with estimating the natural damping in structures, engineers have introduced energy dissipating systems into the design of buildings to provide controllable and specifiable amounts of damping. Structural designers who attempt to solve motion comfort problems in tall structures have found that adding damping directly to the structure is often the most reliable and effective way to limit structural motion. High levels of damping can be obtained through the design of large capacity viscous fluid dampers, viscoelastic dampers, friction devices or tuned-mass dampers. As a separate entity, an energy absorbing system can be designed directly in a process similar to that used for strength and deflection of the structural frame. One can specify the amount of damping required to satisfy a motion criterion, design an energy dissipating system to provide that level of damping, and thereby increase the reliability of the expected performance. This section discusses the criteria related to damper design for wind-excited motion and presents an outline of the design methodology for currently available cost effective systems.

5.2 Habitability Criteria for Wind-Excited Motion

The use of energy dissipating systems to reduce wind effects in buildings is focused on the reduction of the RMS acceleration response of the building. Because this type of motion has traditionally been a problem in tall buildings, most applications of energy dissipating systems occur in buildings over 40 stories in height. Over the past 30 years, buildings have become lighter, and the inherent damping has been reduced with the introduction of flexible cladding and partition

systems. Such "lively" buildings have exhibited undesirable dynamic behavior, which has caused occupant discomfort resulting in specifications for acceptable acceleration levels. A summary of these occupant perception criteria has been presented by Isyumov (1994). The criteria presented and used for the design of a tall building should not be targeted to specific numbers, but should be thought of as specified within acceptable ranges, since the entire design process has large uncertainties associated with it (i.e., wind speed estimations, assumed damping levels, actual building period vs. computed period, etc.).

Since occupant discomfort is strongly dependent on the turbulent and buffeting characteristics of the wind, there presently exists no satisfactory computation procedure to simulate these effects (McNamara et al., 1997). As a result, wind tunnel tests must be utilized to determine estimates of acceleration response levels (ASCE, 1996). The dynamic characteristics of the structure are calculated (period, mass), and an estimate of the natural damping is made based on the type of lateral load resisting system and the materials used in construction. A prediction of acceleration response levels for various assumed damping values can then be made by wind-tunnel experiments, after which the level of damping is selected which satisfies the appropriate design criteria.

5.3 Damper Operation

Energy dissipating systems for the control acceleration levels can be classified as active or passive, and are generally divided into two categories: energy dissipating systems and inertial systems. As mentioned previously, Kareem et al. (1999) have provided an extensive summary of the various types of systems currently being used throughout the world.

Most energy dissipating systems reduce the dynamic response by utilizing the relative displacement between adjacent floors of a building. This implies that the system must be capable of dissipating large amounts of energy through the movement of relatively small inter-story displacements since the performance is related to small, often-recurring storms. For occupant comfort, the response parameter to control is the resonant portion of the RMS acceleration of the dynamic motion. In buildings with a predominant alongwind response, the resonant acceleration is only a part of the total dynamic motion that the structure experiences. Background acceleration can also be significant. In buildings with a predominant acrosswind response, the resonant RMS acceleration component can essentially represent the total dynamic response.

Inertial systems reduce the dynamic response by responding to the dynamic motion at the top of the building. Inertial systems can be conceptually thought of as inputting a force (whose magnitude depends on the inertia mass specified) at the top of the building operating 180 degrees out of phase with the building response. One of the major disadvantages of inertial type systems is that they usually require a significant amount of valuable floor space near the top of the structure.

In either system, only a small amount of additional "effective" damping is usually required to reduce the tower acceleration response to acceptable levels. It should be noted that although the overall alongwind base shear and overturning moments are reduced by the added damping, the reduction for these design parameters is not always as large as the reduction in acceleration response. However, if the governing base shear and overturning moment are from the acrosswind

component, the reduction will be of a similar magnitude as that for the acceleration. As the design of the wind related energy dissipating systems is directed at occupant comfort, and reductions in the life safety demands on the structure are not usually considered.

Hydraulic fluid dampers are compact devices that generate dissipative forces. Unlike viscoelastic solid or fluid dampers that have a strong elastic component, most hydraulic fluid dampers exhibit a viscous behavior. Accordingly, in many applications, the force displacement relation of a hydraulic damper can be easily approximated by $F(t) = Cu(t)$, where C is a frequency independent damping constant which depends on the geometric characteristics of the damper and the viscosity of the fluid, and $u(t)$ is the relative velocity between the damper attachments (Skinner et al., 1993).

An iterative design process results when using energy dissipative systems, which significantly change the building's frequency when added to the building. This frequency change occurs through the introduction of additional stiffness associated with the elastic properties of the viscoelastic and/or hysteretic dissipating systems and has a pronounced effect on the overall building behavior. Response predictions that are both frequency dependent and damping dependent must be generated by the wind tunnel tests for assessment of appropriate design damping levels. In applications where fluid type dampers are used, the change in frequency is much less significant. The fluid damper system can be treated as a purely viscous element solely dependent on the velocity of the inter-story displacements.

5.4 Methodology of Structural Design with Dampers

A simplified outline of the design methodology for designing structures with tuned-mass, viscoelastic and viscous fluid dampers is presented in this section. The following procedures used to determine the structural dynamic properties and wind-excited responses are common for all damper types:

1. Model the structure in three dimensions to determine natural frequencies and f_i and mode shapes f_i; compute the generalized mass of the fundamental translational modes M_i^*.

2. Mass properties should include an allowance for a realistic live load at serviceability conditions.

3. Stiffness properties should include all sources of deformation contributing to the lateral response of the serviceability level.

4. Estimate inherent damping of structure.

5. Select serviceability level response criteria based on building occupancy.

6. Perform wind tunnel tests (high-frequency base balance or aeroelastic) of the structure and generate responses for various levels of damping.

Upon completion of the foregoing procedures, the design of the type of damper selected can proceed. Design methodologies for tuned mass, viscoleastic and viscous-fluid dampers, outlining issues that should be addressed, are presented herein.

5.4.1 Tuned-Mass Damper (TMD) Design Methodology

The issues that must be considered in the design of a TMD or sloshing liquid damper are as follows:

1. Determine the equivalent damping required to meet serviceability criteria.
2. Select the damper mass from a mass ratio vs. equivalent damping chart to provide the required damping increment (equivalent damping required - inherent damping).
3. Retain services of a TMD manufacturer or design specialist for detailed design.
4. Confirm the damper performance by simulating the building response with and without the damper using wind tunnel test wind loads.
5. Preliminary guidelines:
    a. The addition of 3% to 4% of critical damping is usually required for office buildings and 4% to 8% or greater for hotels and apartment buildings.
    b. The damper mass is usually limited to approximately 2% of the first mode generalized mass. Practical design considerations will limit the effective damping provided by TMDs to about 5%.

5.4.2 Viscoelastic Damper Methodology

A simplified outline of the design methodology for designing structures for viscoelastic dampers is as follows:

1. Determine the global damping ratio x that will reduce the building response to an acceptable level as predicted from wind tunnel test results.
2. Determine the effective added stiffness k_d required for added dampers using the modified modal strain energy method as: $k_d = 2xk_s/(h - 2x)$, where h is the damper loss factor which is approximately equal to unity, and k_s is the structural story stiffness without added dampers. If the dampers are in diagonal braces with an angle q to the floor, their required damper storage stiffness is $k' = k_d / \cos^2 q$. The brace stiffness k_b should be larger than the damper stiffness, for example $k_b/k' = 6$.

3. Calculate the required area *A* of the viscoelastic material using *A = k'h/G'*, where *h* is the thickness of the viscoelastic slab and *G'* is the storage shear modulus of the viscoelastic material. Determine *h* from the expected maximum displacement in the damper to ensure the shear strain in the viscoelastic material is less than 75%.

4. Review existing building layout to determine damper placement possibilities.

5. Size the dampers with given locations and number. Check the structural members that are part of the damper bay assembly for 1.2 times the maximum damper force.

6. The damper force can be estimated as: $F_{MAX} = x_{\max} k' \sqrt{1+h^2}$, where x_{max} is the maximum damper displacement.

7. Depending on the geometric distribution of the dampers throughout the structure, levels of effective damping of 10% can be obtained.

5.4.3 Viscous Fluid Damper Methodology

A simplified outline of the design methodology for designing structures with viscous dampers is presented below:

1. Compute the generalized criteria damping for the undamped structure by $C_i^* = w_i M_i^*$, where w_i and M_i^* are the circular frequency and the generalized mass for the i^{th} mode under consideration.

2. Select the desired level of effective damping x_c required and compute the damping constant for all elements in the dissipating system.

3. Locate the viscous damping elements throughout the structure to provide a uniform distribution of damping.

4. Analyze the structure to ensure the distribution and damper properties selected provide the required damping.

5. Investigate the local force effects of all damping elements on the structure.

6. Relatively large amounts of damping can be achieved with viscous dampers. Care must be taken for systems where large amounts of damping are added (x_c> 25%) since a large portion of the dynamic resistance is provided by the damping system.

5.5 Concluding Remarks

With the availability of reliable damping devices capable of dissipating large amounts of energy, a new design tool is available to the structural designer. Past applications in wind engineering have given reliable performance from energy dissipating systems and inertial systems. For seismic engineering, a new era is unfolding. Uncertainties associated with assuming damping levels are eliminated by designing building systems for specific damping levels and reliability of predictions of the building's dynamic response will be greatly improved. Cost implications of the addition of damping systems are very promising. Studies indicate that when properly combined with the design of the lateral stiffness system, significant savings can be achieved.

References

ASCE (1996), "Wind Tunnel Model Studies of Buildings and Structures," ASCE Manuals and Reports on Engineering Practice No. 67.

ATC (1993), "Seminar on Seismic Isolation, Passive Energy Dissipation, and Active Control," *Proc. ATC Seminar*, ATC 17-1.

Boggs, D.W. (1992), "Validation of the aerodynamic model method," *J. of Wind Eng. and Ind. Aero.*, **42**: 1011-1022.

Breukelman, B, Dalgleish, A. and Isyumov, N. (1993), "Estimates of Damping and Stiffness for Tall Buildings," *Proc. of the 7th U.S. National Conference on Wind Engineering*, June, Los Angeles.

Celebi, M. and Safak, E. (1991), "Recorded Seismic Response of Transamerica Building. Part I: Data and Preliminary Analysis," *J. Str. Eng*., ASCE.

Cole, H.A. (1973), "On-Line Failure Detection and Damping Measurement of Aerospace Structures by the Random Decrement Signatures," NASA CR-2205.

Davenport, A.G. and Hill-Carroll (1986), "Damping in Tall Buildings: Its Variability and Treatment in Design," *ASCE Spring Convention*, Seattle: 42-57.

ESDU (1983), *Damping of Structures, Part I: Tall Buildings*, Engineering Science Data Units, Item No. 83009, London.

Fujino, Y., et al. (1992), "Tuned Liquid Dampers (TLD) for Suppressing Horizontal Motions of Structures," *J. of Eng. Mech.*, **101**(10).

Fujita, T. (1991), "Seismic Isolation and Response Control of Nuclear and Non-Nuclear Structures," *Proc. of the 11th International Conference of Structural Mechanics in Reactor Technology*, Tokyo.

Ghanem, R. and Shinozuka, M. (1995), "Structural System Identification I: Theory," *Journal of Engineering Mechanics,* **121**(2): 255-264.

Gurley, K. and Kareem, A. (1995), "On the Analysis and Simulation of Random Processes Utilizing Higher Order Spectra and Wavelet Transforms," *Proc. of the International Conference on Computational Stochastic Mechanics*, A.A. Balkema Press, Netherlands.

Hart, G.C. and Vasudevan, R. (1975), "Earthquake Design of Buildings: Damping," *J. of Str. Div*., ASCE, **101**(ST1): 49-65.

Haviland, R. (1976), "A Study of the Uncertainties in the Fundamental Translational Period and Damping Values for Real Buildings," MIT, Research Report No. 5, Pub. No. R76-12, Dept. of Civil Eng., Cambridge, Mass.

Hoshiya, M. and Saito, E. (1984), "Structural Identification by Extended Kalman Filter," *Journal of Engineering Mechanics*, **110**(12): 1757-1770.

Hudson, D.E. (1977), "Dynamic Tests of Full-Scale Structures," *J. of Eng. Mech. Div*., ASCE, **103**(EM6), 1141-1157.

Isyumov, N. (1994), "Criteria for Acceptable Wind Induced Motions," *Proc. ASCE Structure Congress XII*, Atlanta, GA, 642-647.

Izumi, M., et al. (1993), "Building with Response Control in Japan," *Proc. Structures* Congress '93, Irvine, California.

Jeary, A.P. and Ellis, B.R. (1981), "Vibration Tests of Structures at Varied Amplitudes," *Proc. ASCE/EMD Specialty Conference on Dynamic Response of Structures*, ASCE, Atlanta, GA.

Jeary, A.P. (1986), "Damping in Tall Buildings - A Mechanism and a Predictor," *Earthquake Engineering and Structural Dynamics*, **14**: 733-750.

Jeary, A.P. (1992), "Establishing Non-Linear Damping Characteristics of Structures from Non-Stationary Response Time-Histories," *The Structural Engineer,* **70**(4): 61-66.

Jones, N.P. and Spartz, C.A. (1990), "Structural Damping Estimates for Long-Span Bridges," *J. of Eng. Mech.*, **116**(11): 2414-2433.

Kareem, A. (1978), "Wind Excited Motion of Buildings," thesis presented to Colorado State University at Fort Collins, Colorado, in partial fulfillment of the requirements for the degree of Doctor of Philosophy.

Kareem, A. (1981), "Wind-Excited Response of Buildings in Higher Modes," *J. of Str. Eng*., **107**(ST4): 701-706.

Kareem, A. (1982), "Acrosswind Response of Buildings," *J. of Str. Div.,* **108**(ST4): 869-887.

Kareem, A. (1983), "Mitigation of Wind Induced Motion of Tall Buildings," *J. of Wind Eng. and Ind. Aero*. **11**(1-3).

Kareem, A. (1988), "Aerodynamic Response of Structures With Parametric Uncertainties," *Structural Safety***, 5**: 205-255.

Kareem, A. (1994), "The Next Generation of Tuned Liquid Dampers," *Proc. of the 1st World Conference on Structural Control*, Los Angeles.

Kareem A. and Gurley, K. (1995), "Damping in Structures: Its Evaluation and Treatment of Uncertainty," *J. of Wind Eng. And Ind. Aero.*, **59**(2-3).

Keel, C.J. and Mahmoodi, P. (1986), "Design of Viscoelastic Dampers for Columbia Center Building," *Building Motion in Wind*, ASCE, NY.

Kline, S. and Kareem A. (1995), "Performance of Multiple Mass Dampers Under Random Loading," *J. of Str. Eng*., ASCE, **121**(2).

Loh, and Tsaur (1988), "Time Domain Estimation of Structural Parameters," *Engineering Structures*, **10**: 95-105.

Kareem, A., Kijewski, T. and Tamura, Y. (1999), "Mitigation of Motion of Tall Buildings with Recent Applications," *Wind and Structures* **2**(3):201-251.

Koshika, N., et al. (1992), "Control Effects of Active Mass Driver System During Earthquakes and Winds," *Proc. 1st Int'l Conference on Motion and Vibration Control*.

Kwok, K.C.S. and Melbourne, W.H. (1981), "Wind-Induced Lock-In Excitation of Tall Structures," *J. of Str. Div*., ASCE, **107**(ST1): 57-72.

Lagomarsino, S. (1993), "Forecast Models for Damping and Vibration Periods of Buildings," *J. of Wind Eng. and Ind. Aero.*, **50**: 309-318.

Li, Y. and Kareem, A. (1990a), "Recursive Modeling of Dynamic Systems," *J. of Eng. Mech*., ASCE, **116**(3).

Li, Y. and Kareem, A. (1990b), "ARMA Systems in Wind Engineering," *Prob. Eng. Mech*., **5**(2).

Li, Y. and Kareem, A. (1993), "Parametric Modeling of Stochastic Wave Effects on Offshore Platforms," *Applied Ocean Research*, **15**(2).

McNamara, R.J. (1977), "Tuned Mass Dampers for Buildings," *J. of the Str. Div*., ASCE, **109**(ST9).

McNamara, R.J., Boggs, D.W., Lai, M.L., Makris, N., Nielsen, E.J. and Cermak, J. E. (1997), "Tailoring of Damping in Structures: Design Issues," *Building to Last, Proceedings of Structures Congress XV*, ASCE, Portland, April 13-16, **2**: 1073-1077.

Nashif, A.D., Jones, D.G., and Henderson, J.P. (1984), *Vibration Damping*. John Wiley & Sons.

Novak, M. (1971), "Data Reduction From Nonlinear Response Curves," *J. of Eng. Mech. Div*., ASCE, **97**(EMD): 1187-1204.

Novak, M. (1974), "Effect of Soil on Structural Response to Wind and Earthquake," *Earthquake Eng. and Str. Dyn*., **3**.

Otsuki, Y., Washizu, K., Tomizawa, H. and Ohya, A. (1974), "A Note on the Aeroelastic Instability of a Prismatic Bar With Square Section," *J. of Sound and Vib*., **34**(2): 233-248.

O'Rourke, M.O. (1976), "Discussion on Response of Stochastic Wind of N-Degree Tall Buildings," *J. of Str. Eng.,* ASCE, **102**(ST12): 2401-2403.

Raggett, J.D. (1975), "Estimating Damping of Real Structures," *J. of Str. Div*., ASCE, **101**(ST9): 1823-1835.

Safak, E. (1989), "Adaptive Modeling, Identification and Control of Dynamic Structural Systems," *J. of Eng. Mech*., ASCE, **115**(1).

Sakai, F., et al. (1989), "Tuned Liquid Column Damper - New Type Device for Suppression of Building Vibrations," *Proc. Int'l Conf. on High-Rise Buildings*, Nanjing, China.

Sakamoto, M., and Kobori, T. (1996), "Applications of Structural Response Control," *Proc. of the 2nd Intl Workshop on Structural Control*, IASC, Hong Kong.

Saunders, J.W. and Melbourne, W.H. (1975), "Tall Rectangular Building Response to Cross-Wind Excitation," *Proc. of the 4th Int'l Conference on Wind Effects on Buildings and Structures*, Cambridge University Press, Sept.: 369-379.

Scanlan, R.H. and Tomko, J.J. (1971), "Airfoil and Bridge Deck Flutter Derivatives," *J. of Eng. Mech*., **97**(EM6): 1717-1737.

SEF (1994), "Seismic Damping Devices, Engineers Find Innovative Ways to Increase Structural Damping Properties," *Str. Eng. Forum*, October.

Seismic Design Symposium (1995). *Symposium on a New Direction in Seismic Design*, Tokyo.

Shimizu, K. and Teramura, A. (1994), "Development of Vibration Control System Using U-Tube Water Tanks," *Proc. of Int'l Workshop and Seminar on Behavior of Steel Structures in Seismic Areas*, June-July, Timisoara, Romania.

Shinozuka, M. and Ghanem, R. (1995), "Structural System Identification II: Experimental Verification," *Journal of Engineering Mechanics*, **121**(2): 265-273.

Skinner, R.I., Robinson, W.H., and McVerry, G.H. (1993), *An Introduction to Seismic Isolation*. John Wiley and Sons, New York, NY.

Soong, T.T. (1990). *Active Control: Theory and Practice*, Wiley, New York.

Steckley, A. (1989), "Motion Induced Wind Forces on Chimneys and Tall Buildings," Ph. D. thesis, University of Western Ontario, London, Canada.

Suda, K., Satake, N., Ono, J., and Sasaki, A. (1995), "Damping Properties of Buildings in Japan," *J. of Wind Eng. and Ind. Aero*., **59**(2-3): 383-392.

Suhardjo, J., Spencer, Jr., B.F., and Kareem, A. (1992), "Frequency Domain Optimal Control of Wind Excited Buildings," *J. of Eng. Mech.*, **118**(12).

Tamura, Y. (chairman), Arakawa, T., Morita, K., Ono, J., Sasaki, A., Satake, N. and Suda, K. (1996), *Database of Dynamic Properties of Buildings and Structures in Japan.* Research Committee on Damping Evaluation, Architectural Institute of Japan.

Tamura, Y. (1993), "Recent Topics of Vibration Control for Wind-Induced Vibrations of Buildings," English translation of a paper by Tamura in Japanese in *Proc. of the 2nd Colloquium on Vibration Control of Structures*, JSCE.

Tamura, Y. (1997), "Japanese Damping Database," *Building to Last, Proceedings of Structures Congress XV*, ASCE, Portland, April 13-16, **2**: 1064-1067.

Tamura, Y., et al. (1988), "Wind Induced Vibration of Tall Towers and Practical Applications of Tuned Sloshing Dampers," *Proc. of the Symposium/Workshop on Serviceability of Buildings*, Ottawa, Canada.

Tamura, Y., Sasaki, A., Sato, T., and Kousaka, R. (1992), "Evaluation of Damping Ratios of Buildings During Gusty Wind Using the Random Decrement Technique," *12th Wind Engineering Symposium*.

Tamura, Y., Shimada, K., and Hibi, K. (1993), "Wind Response of a Tower Wind (Typhoon Observation at Nagasaki Huis Ten Bosch Domtoren)," *J. of Eng. And Ind. Aero*., **50**: 309-318.

Tamura, Y., Shimada, K., Sasaki, A., Kohsaka, R., and Fuji, K. (1995), "Variation of Structural Damping Ratios and Natural Frequencies of Tall Buildings During Strong Winds," *Proc. of the 9th Int'l Conf. Of Wind Eng.*, Wiley Eastern, New Delhi.

Tamura. Y. and Suganuma, S.-Y. (1996), "Evaluation of Amplitude-Dependent Damping and Natural Frequency of Buildings During Strong Winds," *J. of Wind Eng. and Ind. Aero.,* **59**(2,3): 115-130.

Tamura, Y., Yamada, M., and Yokota, H. (1994),"Estimation of Structural Damping of Buildings," *ASCE Structures Congress and IASS International Symposium*, Atlanta, **2**: 1012-1017.

Taoka, G.T., Hogan, M., Khan, F. and Scanlan, R.H. (1975), "Ambient Response Analysis of Some Tall Structures," *J. of Str. Eng*., **101**(ST1): 49-65.

Trifunac, M.D. (1972), "Comparisons Between Ambient and Forced Vibration," *Earthquake Eng. and Str. Dyn*, **1**: 133-150.

Vandiver, J.K., Dunwoody, A.B., Campbell, R.B. and Cook, M.F. (1982), "A Mathematical Basis for the Random Decrement Vibration Signature Analysis Technique," *J. of Mech. Design*, **104**: 307-313.

Watanabe, Y., Isyumov, N., and Davenport, A.G. (1995), "Empirical Aerodynamic Damping Function for Tall Buildings," Proc. of the 9th Int'l Conf. On Wind Eng., Wiley Eastern, New Delhi: 1362-1371.

Wolf, J.P. (1988), *Soil-Structure-Interaction Analysis in Time Domain*. Prentice-Hall, Englewood Cliffs, N.J.

Yamazaki, S., Nagata, N. and Abiru, H. (1992), "Tuned Active Dampers Installed in the Minato Mirai (mm) 21 Landmark Tower in Yokohama," *J. of Wind Eng. and Ind. Aero.*, **41-44**.

Yang, J.C.S., Dagalakis, N.G., Everstine, G.C., and Wang, Y.F. (1983), "Measurement of Structural Damping Using the Random Decrement Technique," *Shock and Vibration Bulletin*, **53**(4): 63-71.

Yokoo, Y. and Akiyama, H. (1972), "Lateral Vibration and Damping Due to Wind and Earthquake Effects," *Proc. of the Int'l Conf. On Planning and Design of Tall Buildings*, **II-17**, ASCE, New York.

Yun, C.-B. and Shinozuka, M. (1980), "Identification of Nonlinear Structural Dynamic Systems," *Journal of Structural Mechanics*, **8**(2): 187-203.

2IWSC (1996), "Next Generation of Intelligent Structures," *2nd Int'l Workshop on Structural Contro*l, IASC, Hong Kong.